NASA Technical Paper 3141

November 1991

The Microgravity Environment of the Space Shuttle Columbia Payload Bay During STS-32

Bonnie J. Dunbar,
Robert L. Giesecke,
and Donald A. Thomas

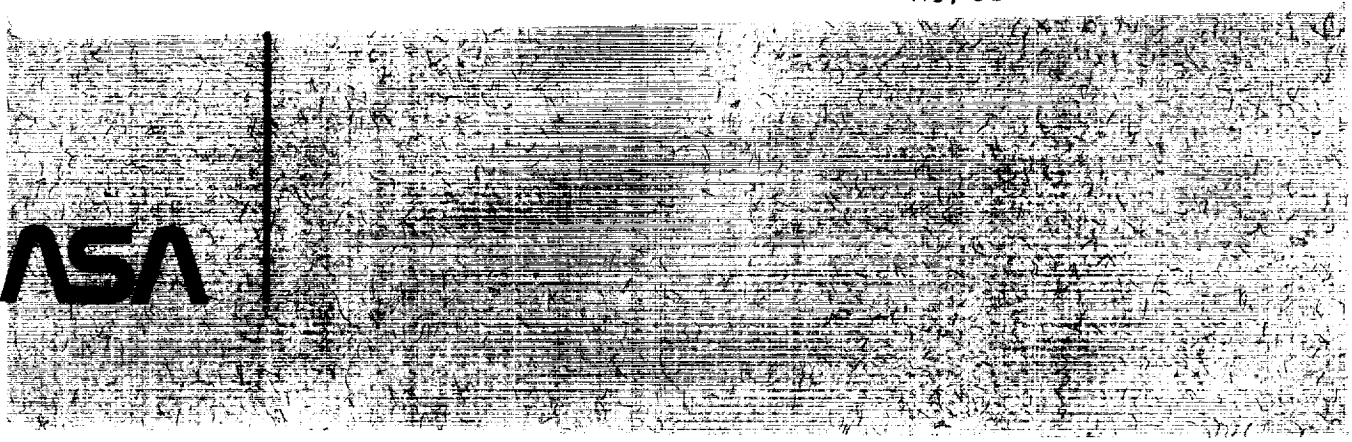

NASA

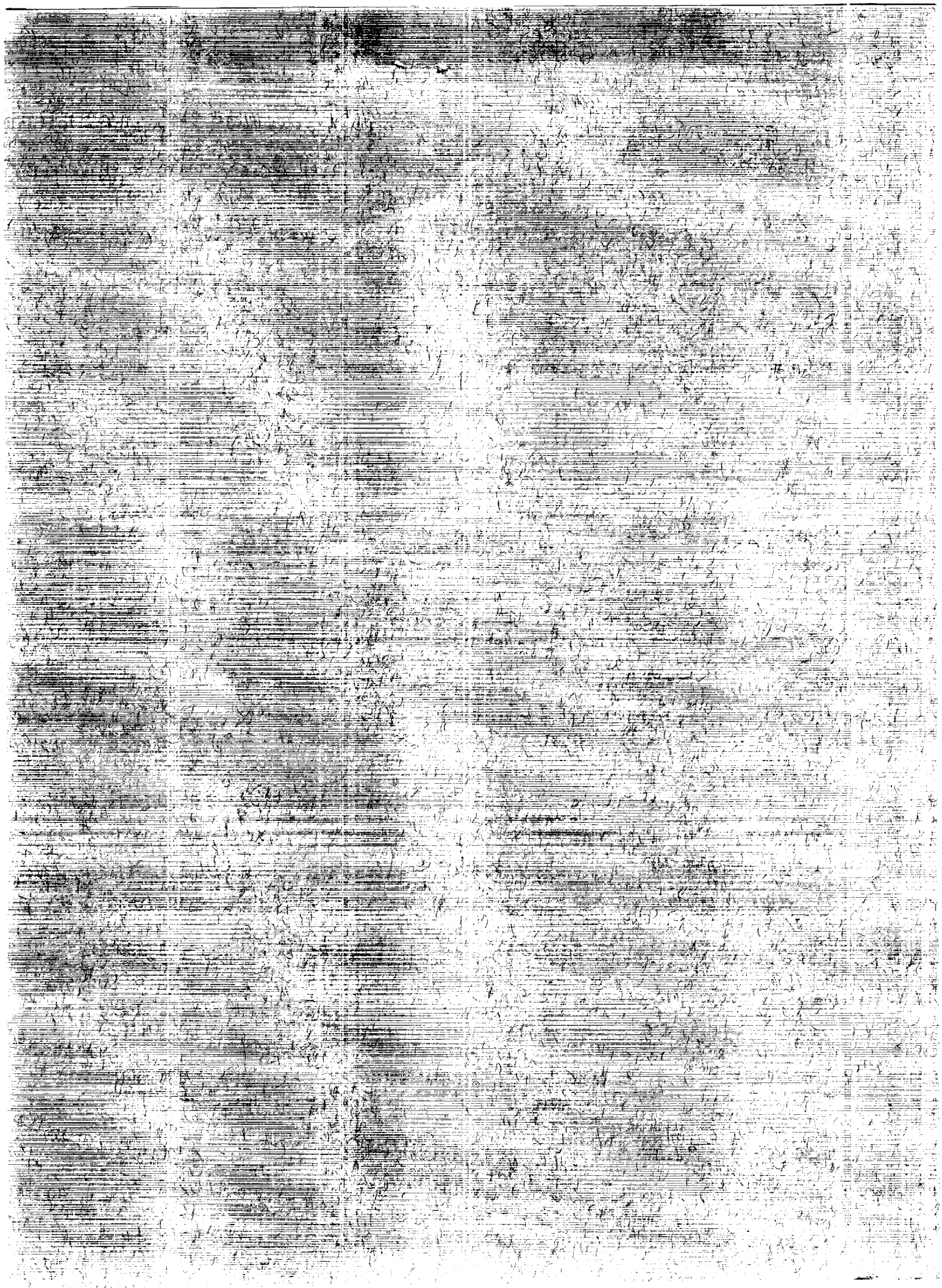

NASA Technical Paper 3141

1991

The Microgravity Environment of the Space Shuttle Columbia Payload Bay During STS-32

Bonnie J. Dunbar,
Robert L. Giesecke,
and Donald A. Thomas
Lyndon B. Johnson Space Center
Houston, Texas

National Aeronautics and Space Administration
Office of Management
Scientific and Technical Information Program

CONTENTS

TABLES

FIGURES

ABSTRACT

Over 11 hours of three-axis microgravity accelerometer data were successfully measured in the payload bay of Space Shuttle Columbia as part of the Microgravity Disturbances Experiment (MDE) on STS-32. The data were measured using the High Resolution Accelerometer Package (HIRAP) and the Aerodynamic Coefficient Identification Package (ACIP) which were mounted on the Orbiter keel in the aft payload bay. Data were recorded during specific mission events such as Orbiter quiescent periods, crew exercise on the treadmill, and numerous Orbiter engine burns. Orbiter background levels were measured in the 10^{-5}g range, treadmill operations in the 10^{-3}g range, and Orbiter engine burns in the 10^{-2}g range. Induced acceleration levels resulting from the SYNCOM satellite deploy were in the 10^{-2}g range, and operations during the pre-entry flight control system (FCS) checkout were in the 10^{-2} to 10^{-1}g range.

INTRODUCTION

Among microgravity scientists, it is well known that the magnitude of residual acceleration aboard an orbiting spacecraft is a critical parameter in conducting materials processing experiments in the reduced gravity environment of space.[1,2,3,4] The terms *weightlessness* and *zero-gravity* that are frequently used to describe the space environment are misnomers and technically incorrect. The gravity level aboard a spacecraft in low Earth orbit is more accurately described as *microgravity* or *micro-g*, which is technically one millionth the gravity level of Earth (10^{-6}g) and describes the extremely low residual gravity levels experienced aboard an orbiting spacecraft. In spite of its recognition as a critical parameter in processing materials in space, very little information on gravity level has been made available to microgravity scientists conducting experiments aboard the Space Shuttle.

This report summarizes the 11.5 hours of three-axis accelerometer data collected during the STS-32 mission of Space Shuttle Columbia (January 1990) as part of the MDE. The HIRAP and ACIP accelerometer data collection was conducted under the Detailed Supplementary Objective (DSO) #0314, "OV-102 Accelerations Data Collection to Support the Microgravity Disturbances Experiment," which was approved for STS-32.

Additional accelerometer data were collected at a second location within the Orbiter (middeck locker MA9F) using the Honeywell In-Space Accelerometer (HISA) and are summarized elsewhere.[5] These two accelerometer data sets, recorded simultaneously but at widely separated locations within the Orbiter (see figure 1), will permit studies to be performed on how disturbances are transmitted through the Orbiter structure and will be a starting point for mapping the microgravity environment of the Orbiter. The results of these future studies will be reported as data analyses progress.

Because of the limited data recording capability available for accelerometer data, only specific mission events (such as Orbiter engine firings, crew exercise periods on the treadmill, and Orbiter background levels) were targeted for recording accelerometer data.

A second report (soon to be issued) will provide more detailed analyses of this data such as shock spectrum and power spectral density analyses.

HARDWARE DESCRIPTION

The two Orbiter payload bay accelerometer systems used to support the MDE were the HIRAP and the ACIP which are mounted to the keel of Space Shuttle Columbia in bay 13 immediately below the aft payload bay (near the longitudinal center of gravity) at Orbiter coordinates $x_o = 1220$," $y_o = -13$," $z_o = 290$," as illustrated in figure 2.

Both the ACIP and HIRAP triaxial linear accelerometers are based on the pendulous mass principle in which acceleration is sensed by a force-rebalance sensor that attempts to null out any induced pendulum motion. Further details of their operation can be found in reference 6. Specifications for the ACIP and HIRAP accelerometers are presented in tables 1 and 2.

To avoid aliasing, the ACIP and HIRAP data are passed through a 20 Hz filter prior to being sampled, digitized, and recorded. The data sampling rate is 113 samples per second. Aliasing is a phenomenon that occurs in sampled data systems when the sampling frequency is not at least two times higher than the highest frequency of the high frequency components of the data being sensed. If this sampling criterion is not met, the offending high frequency components can appear in the final data product as low frequency data having absolutely no relationship to the actual parameter being measured. In addition to the 20 Hz filter, the HIRAP data are also passed through a 2 Hz filter because the HIRAP principal technologist, being interested only in acceleration data ranging from steady state to 2 Hz, specified that those components from 2 Hz to 20 Hz be attenuated at the rate of 12 db per octave. Unfortunately, the X-axis HIRAP data were lost on the STS-32 mission because of a shorted capacitor in the 20 Hz filter.

The ACIP and HIRAP data are digitized into 14-bit data words, thereby resulting in a resolution of one part in 16,383. This is the determining factor in the resolution listed in performance tables 1 and 2.

TABLE 1. ACIP Accelerometer Performance

Parameter	Performance
Manufacturer	Bendix/Guidance Systems Division
Orientation	three-axis orthogonal
Dynamic range	
X-Axis	± 3.0 g
Y-Axis	± 0.5 g
Z-Axis	± 3.0 g
Accuracy	Better than 1% of full scale
Resolution	
X-Axis	3.6×10^{-4}g
Y-Axis	0.6×10^{-4}g
Z-Axis	3.6×10^{-4}g
Frequency response	dc to 20 Hz
Sample data rate	113 Hz

TABLE 2. HIRAP Accelerometer Performance

Parameter	Performance
Manufacturer/model	Bell Aerospace/XI
Orientation	three-axis orthogonal
Dynamic range	
X-Axis	8×10^{-3}g
Y-Axis	8×10^{-3}g
Z-Axis	8×10^{-3}g
Accuracy	Better than 0.125% of full scale
Resolution	
X-Axis	1.0×10^{-6}g
Y-Axis	1.0×10^{-6}g
Z-Axis	1.0×10^{-6}g
Frequency response	dc to 2 Hz
Sample data rate	113 Hz

REVIEW OF ACCELEROMETER DATA

All accelerometer data presented in this report are reported in terms of the Orbiter coordinate system shown below.

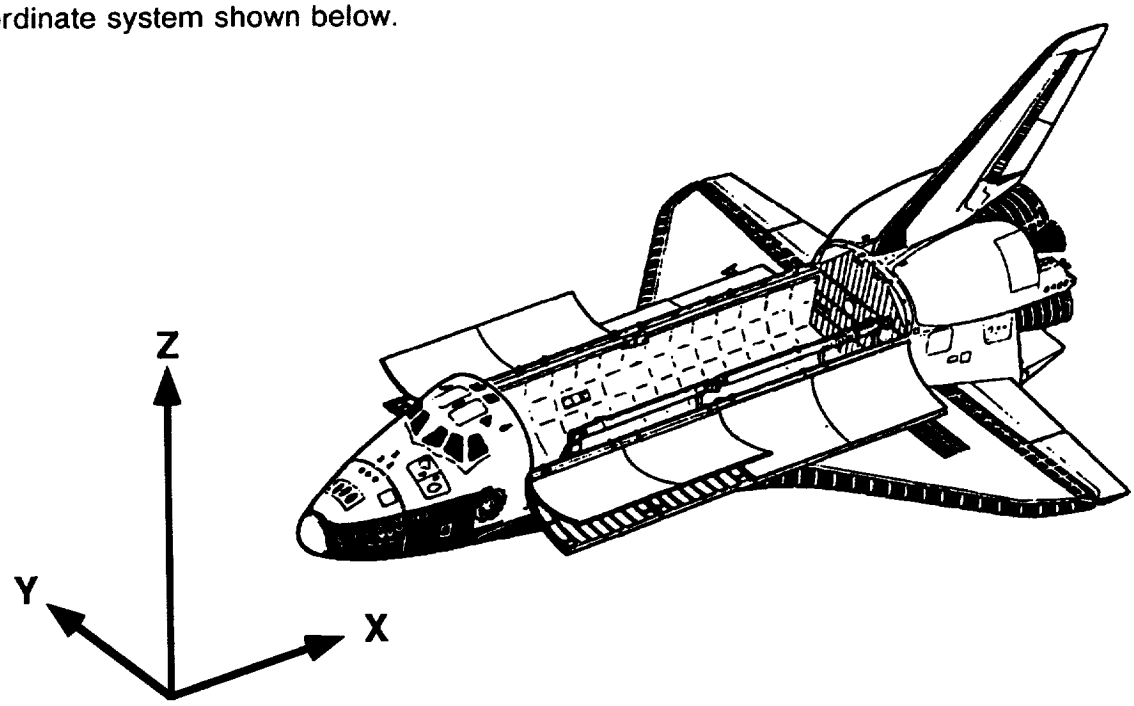

Orbiter Coordinate System

HIRAP/ACIP payload bay accelerometer data were recorded during the STS-32 mission events shown in table 3 (page 5).

Plots 1 through 24 of appendix A show the summary data plots characterizing the three-axis accelerometer levels for each of the events listed in table 3. The accelerometer data are further summarized in table 4 which provides a quick reference of the typical acceleration levels recorded for each of the mission events.

TABLE 3. HIRAP/ACIP Data Summary

1. Rendezvous Orbiter Engine Burns
   - NH1
   - NSR
   - NC4
   - NH2
   - NC5
   - NCC
   - TI

2. SYNCOM Deploy
   - Maneuver to Deploy
   - Deploy
   - Maneuver-to-Separate Burn
   - Separation Burn

3. Exercise Treadmill Activity
   - Commander

4. Proximity Operations Prior to Long Duration Exposure Facility Grapple

5. Water Dump Operations

6. Quiescent Period

7. Inertial Measurement Unit Maneuvers and Alignment

8. Miscellaneous Crew Activity

9. Flight Control System Checkout
   - Auxiliary Power Unit (APU) Startup
   - Elevon Checkout
   - Actuator Checkout

TABLE 4. Summary of Payload Bay Accelerations
(all data reported in units of 1g, normal Earth gravity)

	X-axis	Y-axis	Z-axis
Orbiter background		1.2×10^{-5}	1.5×10^{-5}
Treadmill operations			
Walking			
Commander	6×10^{-4}	2×10^{-4}	1×10^{-3}
Pilot (5.5 mph)	4×10^{-4}	4×10^{-4}	1×10^{-3}
Pilot (2.5 mph)	3×10^{-4}	4×10^{-4}	7×10^{-4}
Pilot (1.5 mph)	3×10^{-4}	4×10^{-4}	6×10^{-4}
Running			
Commander	7×10^{-4}	6×10^{-4}	1.5×10^{-3}
Pilot	9×10^{-4}	7×10^{-4}	1.8×10^{-3}
Orbiter engine burns			
VRCS	1×10^{-4} to 2×10^{-4} along axis of engine firing.		
PRCS			
NC4	1.5×10^{-2}	1.5×10^{-2}	3.8×10^{-2}
NC5	1.3×10^{-2}	1.5×10^{-2}	5.1×10^{-2}
NH2	2.3×10^{-2}	2.0×10^{-2}	7.0×10^{-2}
NCC	1.8×10^{-2}	1.4×10^{-2}	6.7×10^{-2}
TI	2.3×10^{-2}	2.0×10^{-2}	7.0×10^{-2}
SYNCOM MNVR TO SEP	1.0×10^{-2}	1.3×10^{-2}	3.1×10^{-2}
OMS			
NH1	4.3×10^{-2}	2.3×10^{-2}	3.8×10^{-2}
NSR	4.1×10^{-2}	1.0×10^{-2}	3.7×10^{-2}
SYNCOM SEP	4.0×10^{-2}	2.4×10^{-2}	3.4×10^{-2}
SYNCOM deploy	1.1×10^{-2}	2.3×10^{-2}	3.3×10^{-2}
APU startup	2×10^{-3}	8×10^{-3}	2×10^{-2}
Elevon movement	6×10^{-3}	1×10^{-2}	4×10^{-2}
Actuator closings	2×10^{-2}	2×10^{-2}	9×10^{-2}

ORBITER BACKGROUND LEVELS

Plot 1 of appendix A illustrates the "background" microgravity levels recorded in the Orbiter payload bay during normal Shuttle operations on STS-32. These low background levels were within the noise regime of the ACIP accelerometers, and only the more sensitive HIRAP accelerometers provided useful information. As mentioned previously, the X-axis HIRAP accelerometer was not functional, so only Y and Z axes accelerometer data are available for the aft payload bay. As there is large scatter in the peak accelerations (see the time-history plots in appendix A), only typical or average peak acceleration levels are reported here. A more detailed analysis of the data focusing on peak accelerations and averages at various frequencies is in progress.

The background acceleration levels measured were typically in the 1.0×10^{-5}g to 1.5×10^{-5}g range for the Orbiter Y and Z axes, respectively. Similar to measurements made with the HISA middeck accelerometer,[5] the Z-axis has the highest background acceleration levels. No accurate information on the DC acceleration levels can be obtained from the HIRAP or ACIP data at this time due to data offsets resulting from fluctuations in temperatures and temperature gradients in the accelerometers.

Examination of the frequency content of these data indicates that the 17 Hz vibration of the Orbiter due to dither in the Ku band antenna was present, but not as predominant as it was when measured by the middeck accelerometers which were mounted much closer to the Ku band antenna.

SUPPLY WATER DUMP

Approximately 1 hour of accelerometer data were collected during Orbiter water supply dump operations. The induced acceleration levels from the water dump were below the detection capability of the ACIP accelerometers and within the background noise levels of the Orbiter as measured with the HIRAP accelerometers, and are estimated to be below 1×10^{-5}g.

CREW TREADMILL ACTIVITY

Plots 2 and 3 of appendix A illustrate the microgravity levels induced in the payload bay during crew activity on the exercise treadmill. (NOTE: The "square" feature of the data in the X and Z axes of plot 2 are due to the lower sensitivity and resolution of the ACIP as compared to HIRAP. This data is near the detection capability of the instrument.) The treadmill was mounted to the floor of the middeck in front of the airlock--roughly 59 feet from the HIRAP/ACIP accelerometers. Accelerometer data were collected on two of the three crewmembers (commander and pilot) who performed treadmill exercise.

Expanded in more detail, plot 4 compares the characteristic Z-axis patterns of the two crewmembers running. While the middeck accelerometers showed different and distinct

induced acceleration patterns for each crewmember, the payload bay accelerometers measured very little difference between runners. The 2 to 3 Hz characteristic frequency due to the natural running pace of treadmill exercise was not detected by the payload bay accelerometers as it was in the middeck.

Overall, the greatest induced accelerations for these crewmembers were along the Orbiter Z-axis which is perpendicular to the plane of the treadmill. These Z-axis accelerations were typically measured to be 1×10^{-3}g to 2×10^{-3}g. Induced accelerations along the X and Y axes were roughly two times lower in magnitude than along the Z-axis. (NOTE: Because of the wide range in the acceleration levels measured during treadmill operations, only "typical" acceleration levels representative of most of the data collected are reported here. Maximum and minimum acceleration levels recorded for these events can be obtained by further examination of the data plots in appendix A.)

ORBITER ENGINE BURNS

During the STS-32 mission, the acceleration levels induced in the payload bay from at least 12 Orbiter engine burns were successfully recorded with the HIRAP/ACIP. These included three Vernier Reaction Control System (VRCS) engine firings, six Primary Reaction Control System (PRCS) burns, and three Orbiter Maneuvering System (OMS) burns which are listed in table 5 along with their resulting changes in Orbiter velocity, Δv_x, Δv_y, and Δv_z.

Appendix B contains further details of the OMS and RCS engine systems along with a description of the burns listed in table 5.

TABLE 5. STS-32 Orbiter Engine Burn Parameters

Burn type	**Change in velocity** (feet per second)		
	Δv_x	Δv_y	Δv_z
VRCS	(typically less than 0.01)		
PRCS			
NH2	2.6	0.0	0.0
TI	-0.2	0.1	-3.4
NC4	2.2	0.0	0.0
NC5	-1.2	0.0	0.0
NCC	0.6	-0.03	0.8
OMS			
NH1	-7.2	0.1	0.0
NSR	9.4	-0.1	0.0
SYNCOM SEP	17.3	-0.1	-5.4

Vernier RCS

Plot 5 illustrates the induced accelerations resulting from a single-axis vernier jet firing. The resulting induced accelerations are principally along the single axis of the burn with the other axes relatively unaffected. This burn lasted about 2 seconds and produced approximately a 2×10^{-4}g acceleration for the duration of the burn. Very little transients were associated with this burn, with the induced accelerations dropping rapidly at the conclusion of the burn. (NOTE: The 1×10^{-4}g offsets in the acceleration levels are due to temperature fluctuations that introduce a bias in the HIRAP accelerometer.)

Plots 6 and 7 illustrate the induced accelerations resulting from multi-axis vernier burns. The response of the Orbiter to these engine firings is very similar to the single-axis engine burn, although transients and exponential damping of the signal is more evident at the conclusion of these burns.

Primary RCS

Plots 8 through 16 illustrate the induced accelerations in the Orbiter payload bay resulting from the firing of PRCS engines. Five of the burns (NC4, NH2, NC5, NCC, and TI) were associated with the Long Duration Exposure Facility (LDEF) rendezvous sequence and occurred on mission day 4. The maneuver-to-separate burn was performed on mission day 2 after deployment of the SYNCOM satellite. The acceleration time-history plots illustrate the short duration of the individual thruster firings that make up these complex maneuvers and the resulting "ringing" and transient exponential decay in acceleration experienced in the Orbiter structure. Following each firing, there is about a 15-second decay time until the acceleration levels approach the original pre-burn background levels once again.

PRCS engine burns produced Orbiter accelerations in the 1×10^{-2} to 7×10^{-2}g range as measured in the payload bay. Three distinct modes of thruster firings are evident from the PRCS acceleration traces shown in plots 8 through 16. These include:

- Continuous Thruster Firing. This mode is demonstrated in plots 8 and 11 for the NC4 and NH2 burns (X-axis). These burns appear similar to OMS firings in that the induced accelerations resemble a "square" wave function, with a sharply defined step increase at engine firing (1 to 10 seconds) followed by a rapid step decrease at the conclusion of the engine burn (engine shutdown). As with the OMS burns, there is some exponentially damped oscillatory "ringing" in the acceleration level during the constant thrust portion of the event.

- Pulse Firing Mode. Examples of the pulse firing mode are illustrated in plots 8 through 15, with the best example in the NC5 burn shown in plot 10. The burn sequence consists of a series of individual short-duration pulses, each of which produces a spike in the acceleration traces. Some of the burn sequences illustrated here consist of 10 to 20 of these individual pulses.

- Combination Mode. The X-axis accelerometer trace of the TI burn (plot 16) illustrates the combination mode PRCS firing. During the 10-second interval from 30 to 40 seconds, there is a continuous firing in the negative-x direction producing the square wave pattern characteristic of the continuous mode. Superimposed on this pattern are approximately five additional pulse mode engine firings known as pitch axis attitude deadband firings which occur when the Orbiter drifts into a deadband when the digital autopilot is engaged.

Following each individual engine firing of these burn sequences, exponentially damped oscillatory "ringing" in the acceleration level is observed characteristic of the 5.2 Hz first longitudinal bending mode in the X and Z axes of the Orbiter. Further frequency content studies to be performed in the future will investigate the Orbiter structural modes excited by these disturbances.

OMS

The induced acceleration profile of an OMS burn as measured in the Orbiter payload bay can be roughly described by a square wave function as shown in plots 17 through 19 in appendix A for the NH1, NSR, and SYNCOM SEP burns. The OMS engines ignite, produce a constant thrust level (or acceleration) for a fixed duration (10 to 20 seconds), and then abruptly shut down at the end of the scheduled burn period. There is an initial short-duration spike in the acceleration level at the start of the OMS burn (at the leading edge of the square wave function) along each of the Orbiter axes. The magnitudes of these spikes are roughly 4×10^{-2}g, and they appear to last for only a fraction of a second.

The induced accelerations for these OMS burns are greatest along the Orbiter X-axis. After the initial spike at engine startup, the acceleration levels for the three OMS burns measured were 3×10^{-2}g, 7×10^{-3}g, and 7×10^{-3}g, respectively, along the X, Y, and Z Orbiter axes.

There is also some "ringing" associated with the initial startup of the engines which exponentially decays during the burn, followed by additional ringing at the conclusion of the burn (engine shutdown).

As shown in each of the three OMS engine firing plots, the OMS burns are typically followed by PRCS burns for fine-tuned adjustments to the desired burn parameters. The induced disturbances from these PRCS firings are typically 2×10^{-3} to 2×10^{-2}g and are similar in appearance to the PRCS burns discussed previously (NC4, NC5, NH2, NCC, and TI).

SYNCOM SATELLITE DEPLOY

Plot 20 illustrates the induced accelerations during the deployment of the SYNCOM satellite from the Orbiter payload bay on mission day 2. The SYNCOM satellite weighed

15,316 pounds and was deployed a few feet from the HIRAP/ACIP accelerometer systems (SYNCOM coordinates xo = 1206", $y_o = 0.4$", $z_o = 403$").

The satellite was deployed in what is called a "Frisbee" style deployment during which it was released along the positive-z direction in a spinning mode. As expected from this mode of deployment, the maximum induced accelerations were along the Orbiter Z-axis and were measured to be 3×10^{-2}g. The short-duration acceleration spike induced "ringing" and transient exponential decay similar to that observed following PRCS burns (see plots 8 through 16). The frequency content of this ringing is approximately 5 Hz which is one of the primary structural modes of vibration of the Orbiter. Induced accelerations along the X and Y axes were measured to be 1.1×10^{-2} and 2.3×10^{-2}g, respectively.

FLIGHT CONTROL SYSTEM CHECKOUT

Plots 21 through 24 detail some of the induced accelerations that resulted during the flight control system (FCS) checkout of the Orbiter which typically occurs one day before the scheduled landing. Plot 21 illustrates the responses of the Orbiter to the startup of a single APU. This event generated a 2×10^{-2}g acceleration pulse along the Orbiter Z-axis which created a transient exponentially decaying signal similar to that for a single PRCS engine burn or the SYNCOM satellite deploy (plots 10 and 20).

Shortly after APU startup, the left inboard elevon checkout was conducted by cycling the elevon up and down to circulate the hydraulic fluid. A sharp peak in acceleration level of 3×10^{-2} to 4×10^{-2}g along the Orbiter Z-axis was measured each time the elevon movement started or stopped. The induced acceleration pattern during this test is shown in plot 22 which is expanded in more detail in plot 23. The dominant frequency during this test was measured to be about 15 Hz.

The final event of the FCS checkout sequence that was recorded was the actuator checkout shown in plot 24. A series of eight actuator tests involving the aero-surfaces and Space Shuttle main engine actuators are performed which have been reported by Shuttle crews to create quite a loud "bang." These actuator valve closings were measured to induce a sharp acceleration pulse of 1×10^{-1}g along the Orbiter Z-axis which rapidly decayed, once again similar to the PRCS engine burn response. This signal appears to be characteristic of all short-duration, high-magnitude accelerations that are created on the Orbiter.

CONCLUSIONS

Eleven hours of three-axis microgravity accelerometer data were successfully measured in the aft payload bay as part of the MDE on STS-32 using the ACIP and HIRAP accelerometer packages. Orbiter background levels were measured to be in the 10^{-5}g range, treadmill operations in the 10^{-4}g range, and major Orbiter engine burns in the 10^{-2}g range. The deployment of the SYNCOM satellite induced accelerations in the Orbiter

structure in the 10^{-2}g range. APU startup and Orbiter elevon movement during the FCS checkout produced accelerations in the 10^{-2}g range. The largest acceleration measured during orbital operations was in the 10^{-2} to 10^{-1}g range during actuator closings as part of the FCS checkout. Further analysis of the data is in progress and will be reported at a future date.

FUTURE DIRECTIONS

As mentioned previously, three-axis accelerometer data were measured simultaneously with the ACIP and HIRAP using the HISA which was mounted on the Fluids Experiment Apparatus in the Orbiter middeck. Data from this accelerometer are summarized elsewhere.[5] An additional report will be issued comparing the accelerometer measurements made from these widely separated Orbiter locations to investigate how disturbances are transmitted through the Orbiter structure. This is a necessary starting point in mapping the microgravity environment throughout the Orbiter.

REFERENCES

1. R. J. Naumann, "Susceptibility of Materials Processing Experiments to Low-Level Accelerations," N82-12118.

2. B. Feuerbacher, H. Hamacher, R. Jilg, "Compatibility of Microgravity Experiments with Spacecraft Disturbances," Z. Flugwiss. Weltraumforsch 12 (1988), pp. 145-151.

3. F. Gonzalez, J. Merlet, A. Girard, M. R. Razafimaharolahy, "Microvibrations Measurements: A Guarantee of Microgravity Quality for Materials Science Research," Proceedings of 6th European Symposium on Materials Sciences Under Microgravity Conditions, Bordeaux, France, December 2-5, 1986, ESA SP-256, February 1987, pp. 445-451.

4. J. Iwan, D. Alexander, Charles A. Lundquist, "Residual Motions Caused by Micro-Gravitational Accelerations," The Journal of Astronautical Sciences, Volume 35, April - June 1987, pp. 193-211.

5. B. J. Dunbar, D. A. Thomas, J. N. Schoess, "The Microgravity Environment of the Space Shuttle Columbia Middeck During STS-32," NASA TP 3140, September 1991.

6. C. Cooke, et al., SDI Space Shuttle Based Experiments for Acquisition, Tracking, and Pointing (definition of the Space Shuttle Operational Environment), Draper Labs Task 1 final report for Jet Propulsion Laboratory, April 15, 1986.

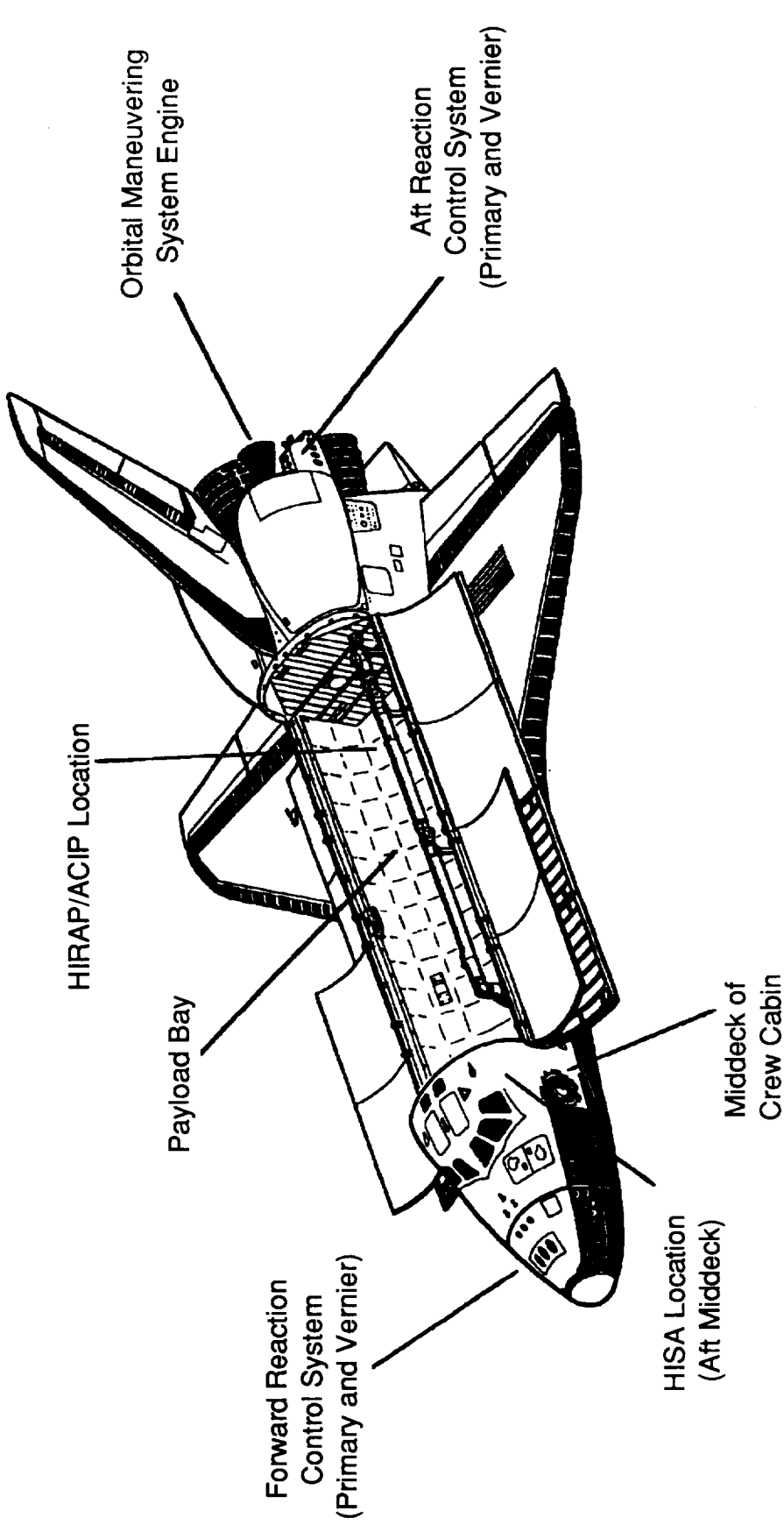

Figure 1. Space Shuttle Orbiter Overview

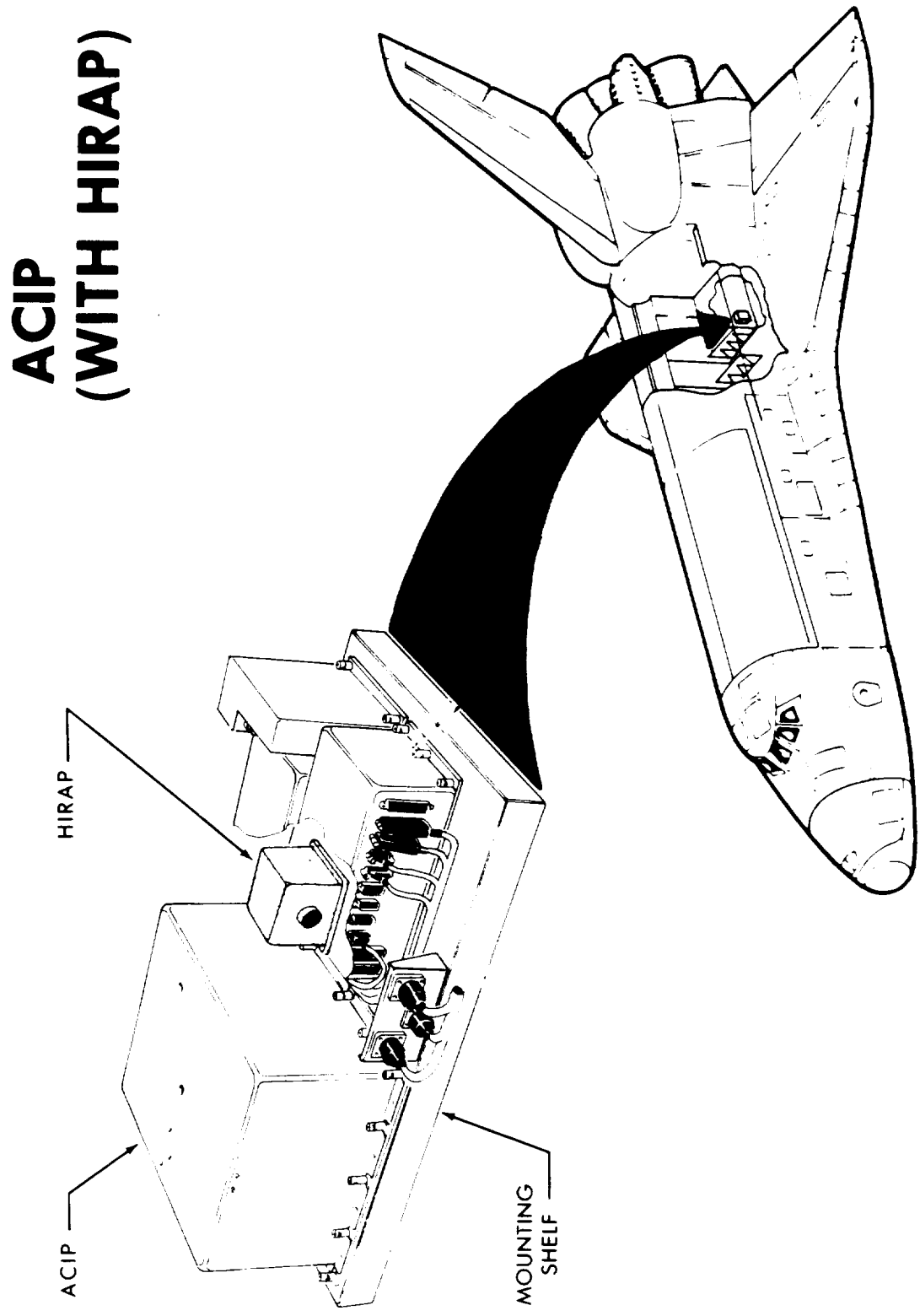

Figure 2. Location of the HIRAP/ACIP accelerometers on the port side of the Orbiter keel, Bay 13.

APPENDIX A

HIRAP/ACIP Accelerometer Data Plots

1. Orbiter Background - HIRAP
2. Treadmill Activity - Commander - ACIP
3. Treadmill Activity - Pilot - ACIP
4. Treadmill Profiles - ACIP
5. Vernier Engine Burn - single-axis - HIRAP
6. Vernier Engine Burn - multi-axis - HIRAP
7. Vernier Engine Burn - multi-axis - HIRAP
8. PRCS Burn - NC4 (part I) - ACIP
9. PRCS Burn - NC4 (part II) - ACIP
10. PRCS Burn - NC5 - ACIP
11. PRCS Burn - NH2 - ACIP
12. PRCS Burn - NCC - ACIP
13. PRCS Burn - MNVR TO SEP (part I) - ACIP
14. PRCS Burn - MNVR TO SEP (part II) - ACIP
15. PRCS Burn - MNVR TO SEP (part III) - ACIP
16. PRCS Burn - TI - ACIP
17. OMS Burn - NSR - ACIP
18. OMS Burn - NH1 - ACIP
19. OMS Burn - SYNCOM SEP - ACIP
20. SYNCOM Deploy - ACIP
21. APU Startup - ACIP
22. Elevon Checkout - ACIP
23. Elevon Checkout - expanded detail - ACIP
24. Actuator Checkout - ACIP

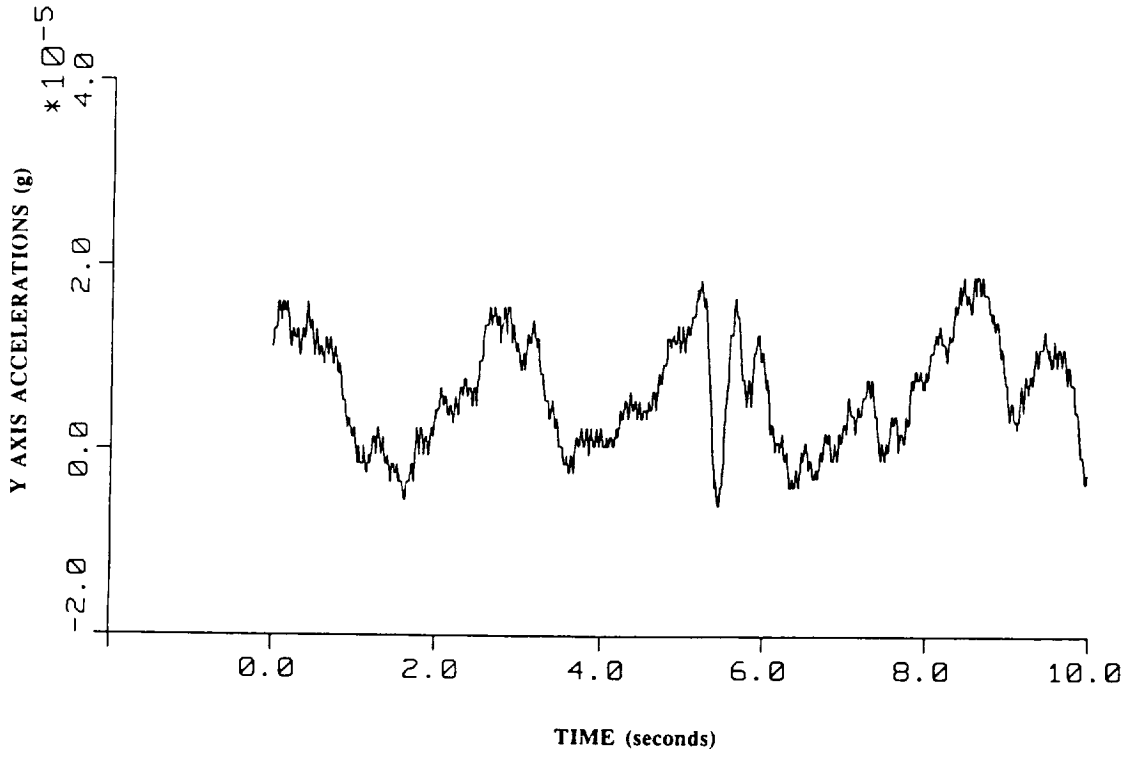

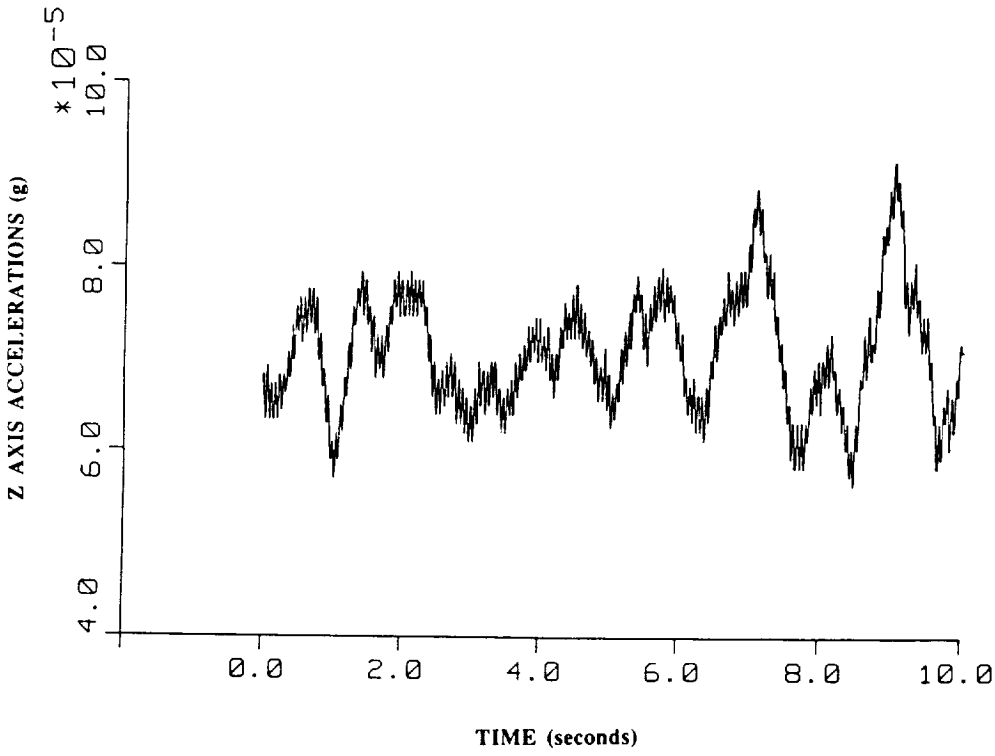

Orbiter Background - HIRAP

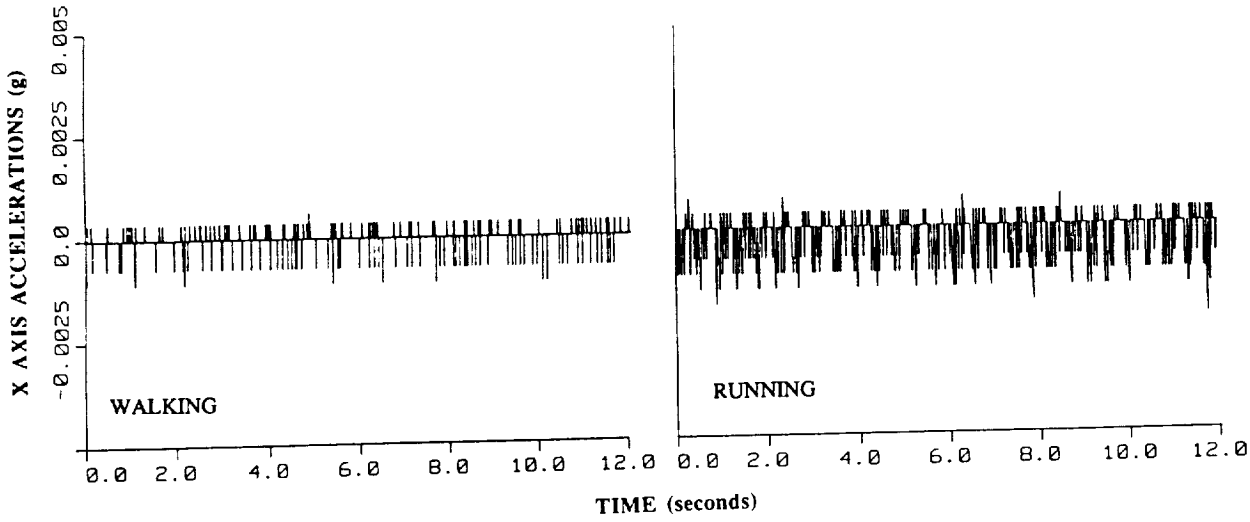

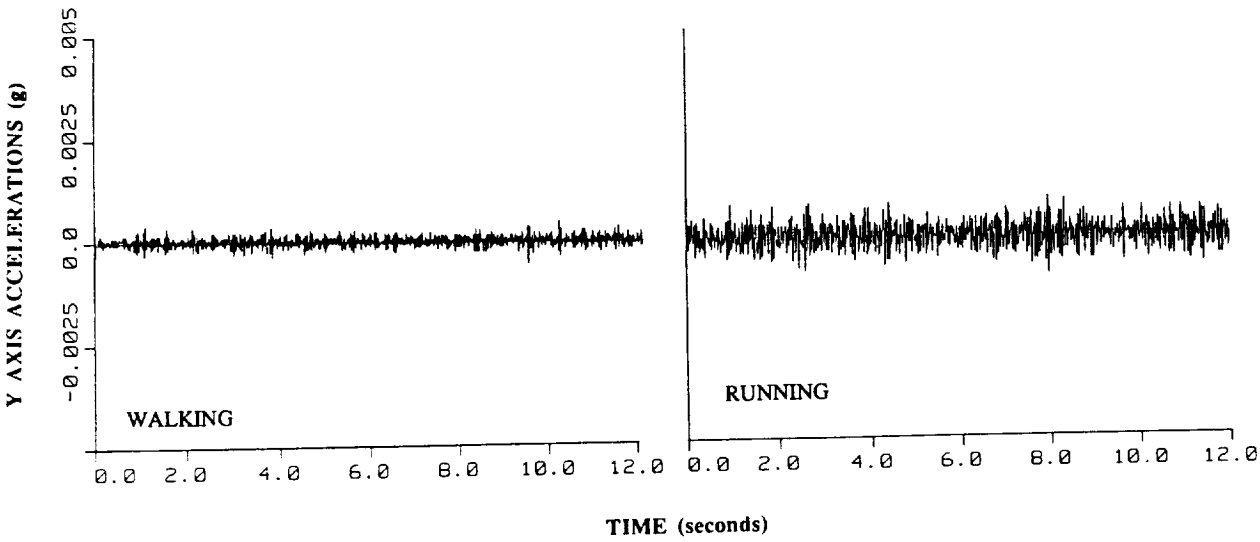

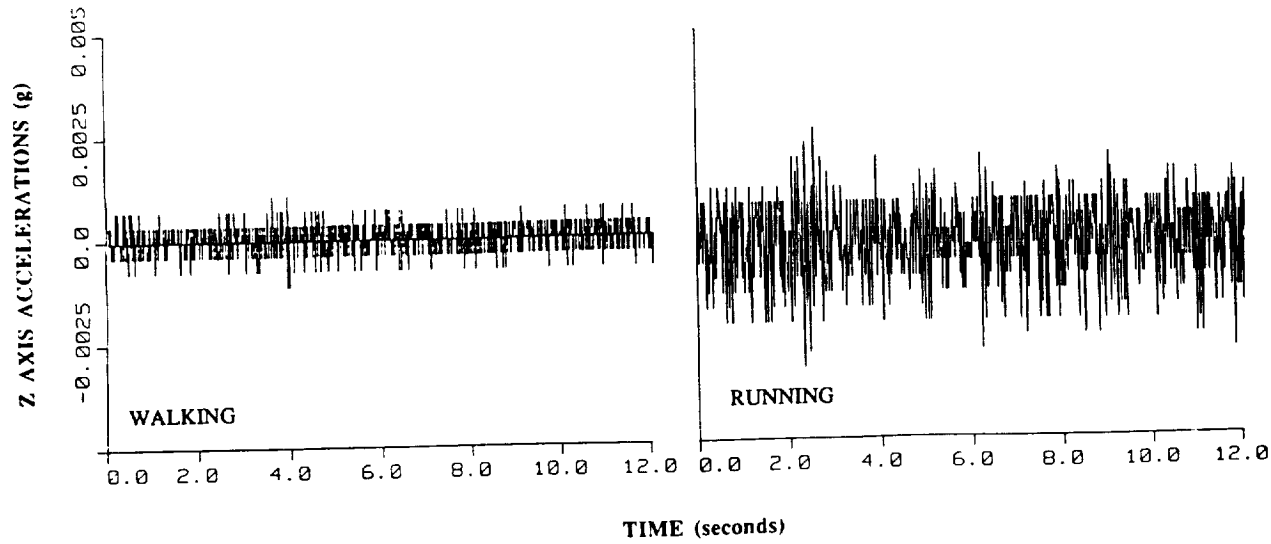

Treadmill Activity - Commander - ACIP

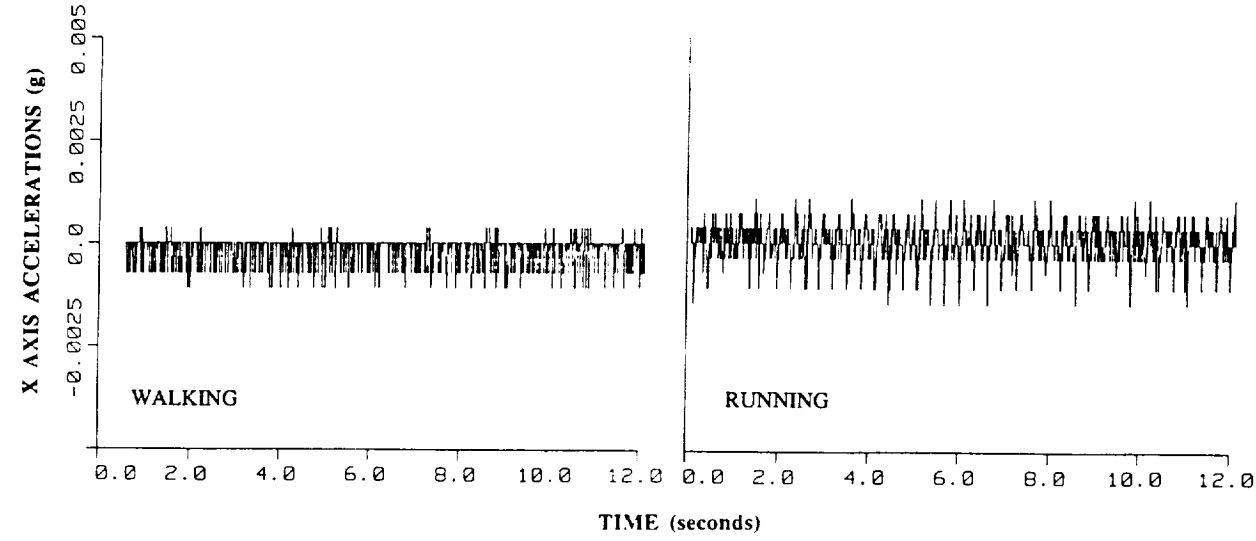

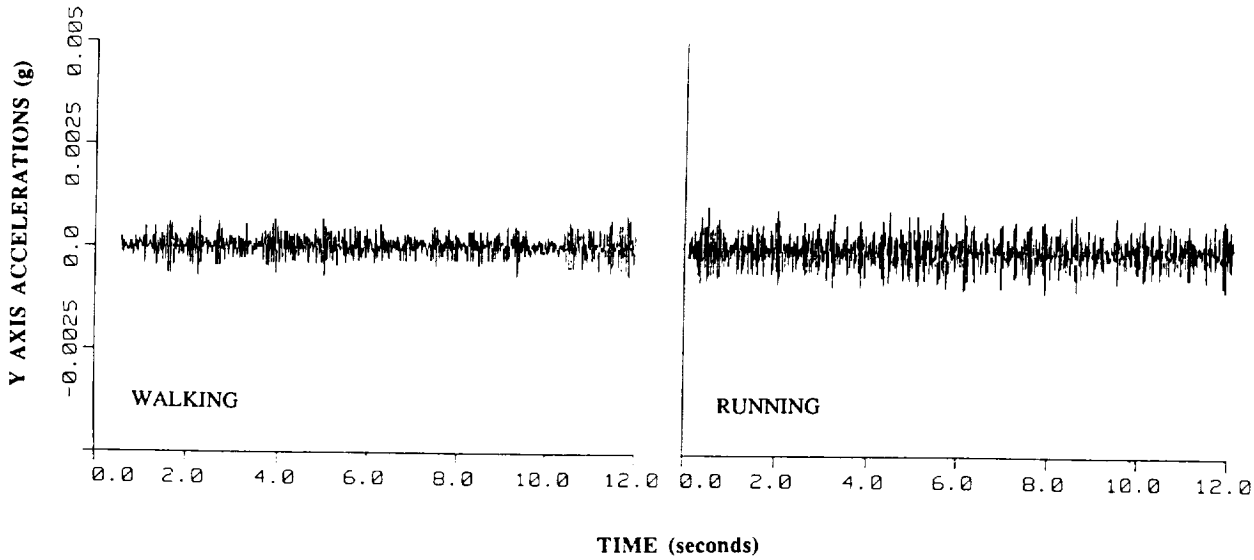

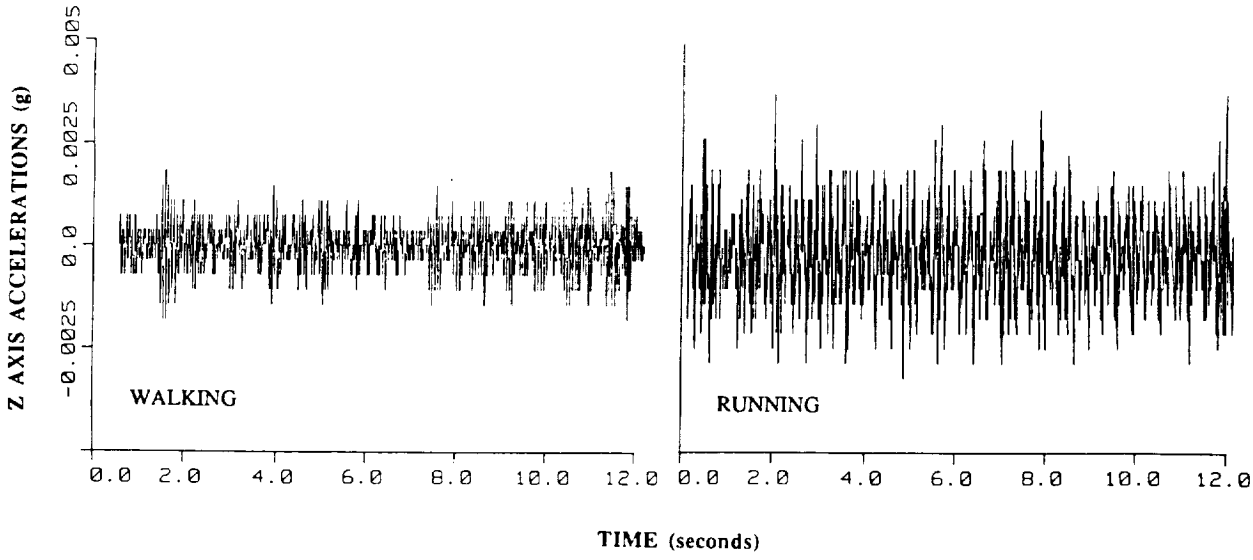

Treadmill Activity - Pilot - ACIP

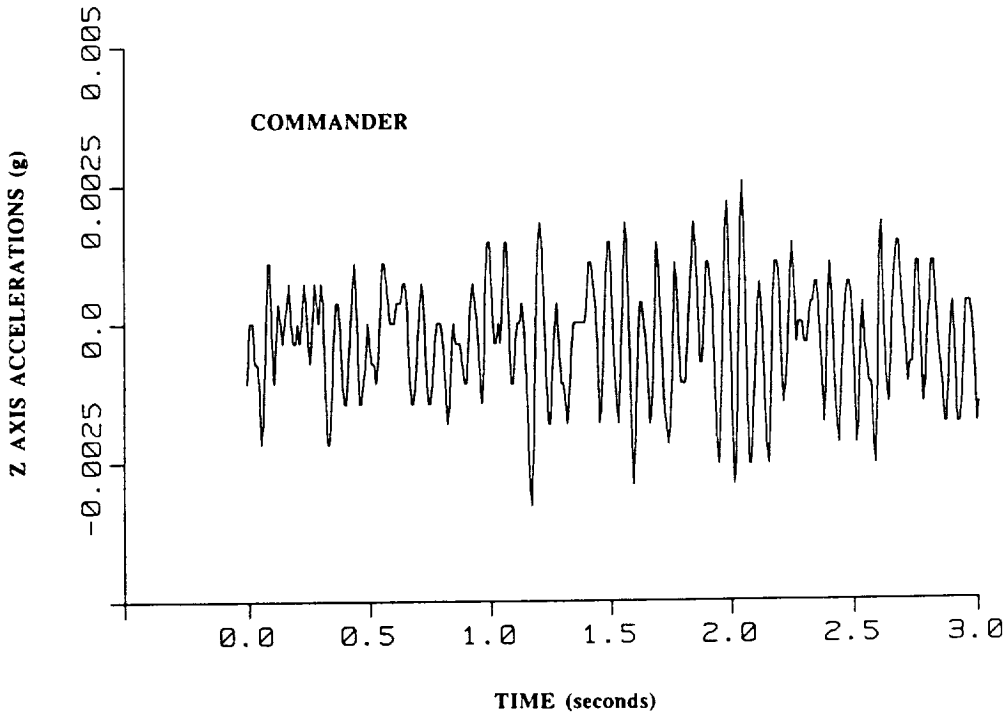

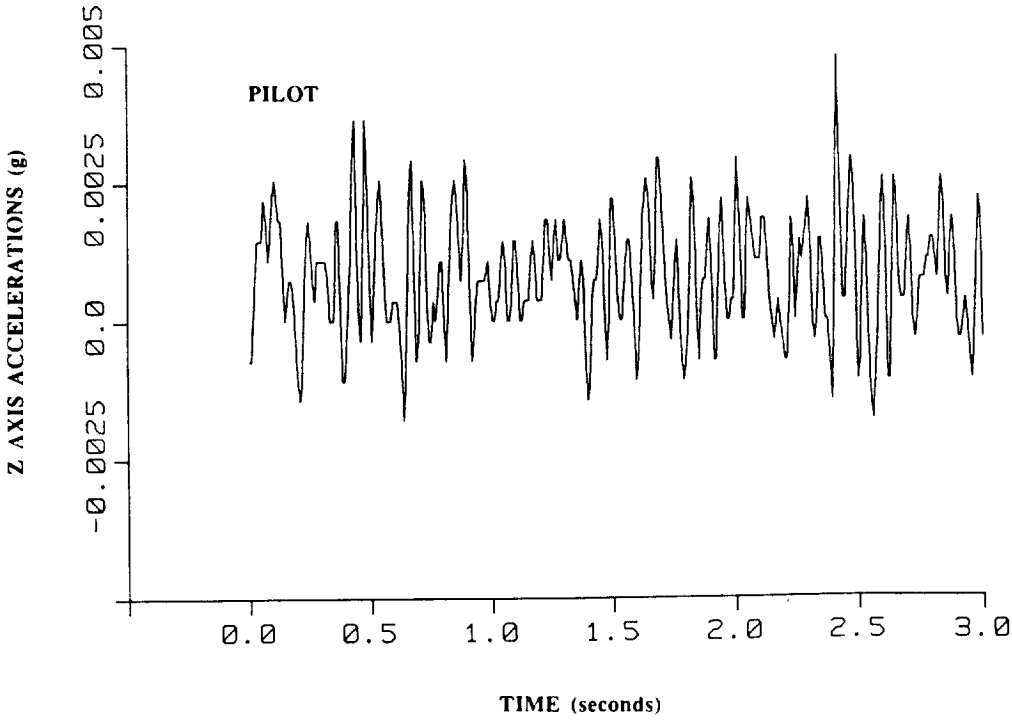

Treadmill Profiles - ACIP

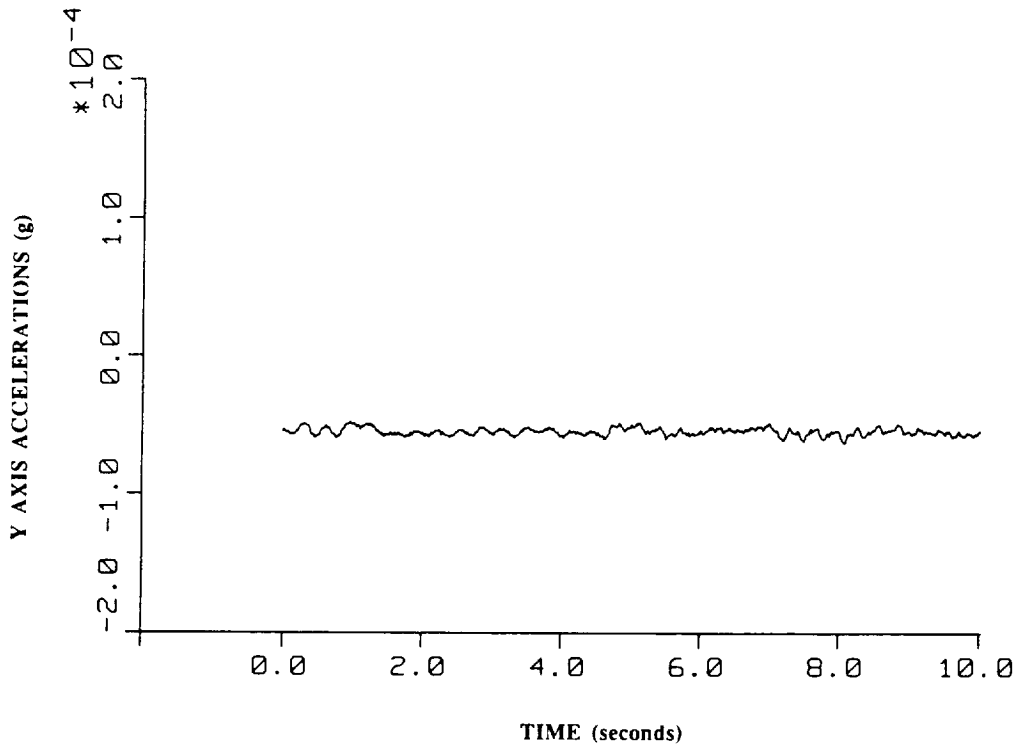

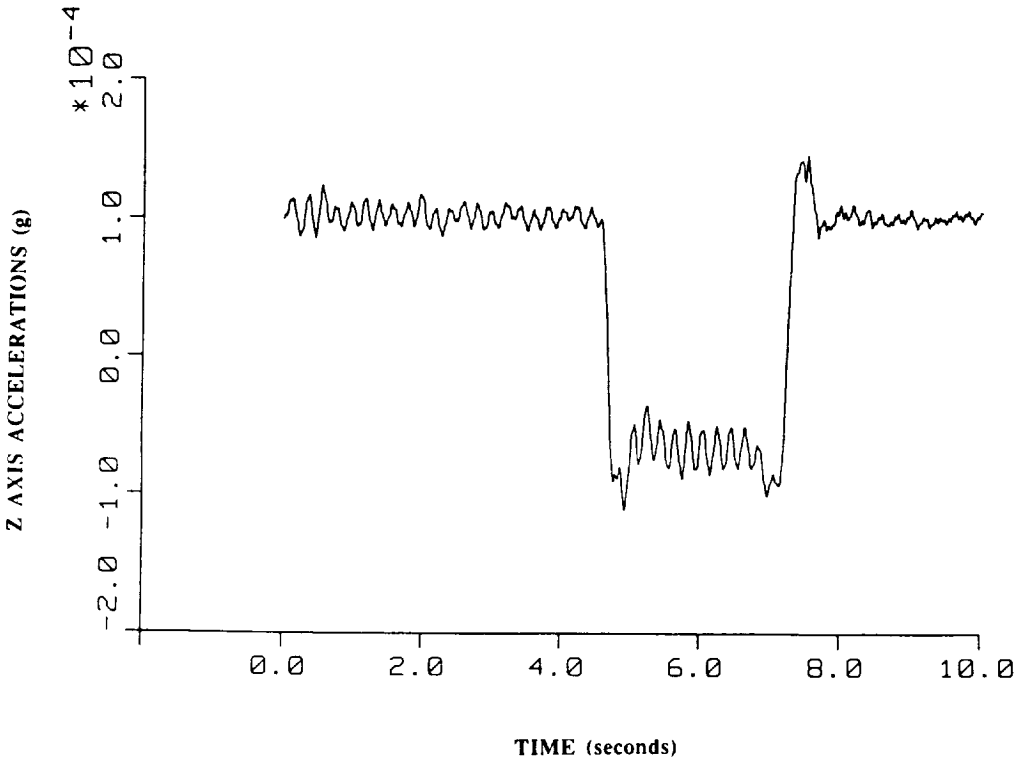

Vernier Engine Burn - single-axis - HIRAP

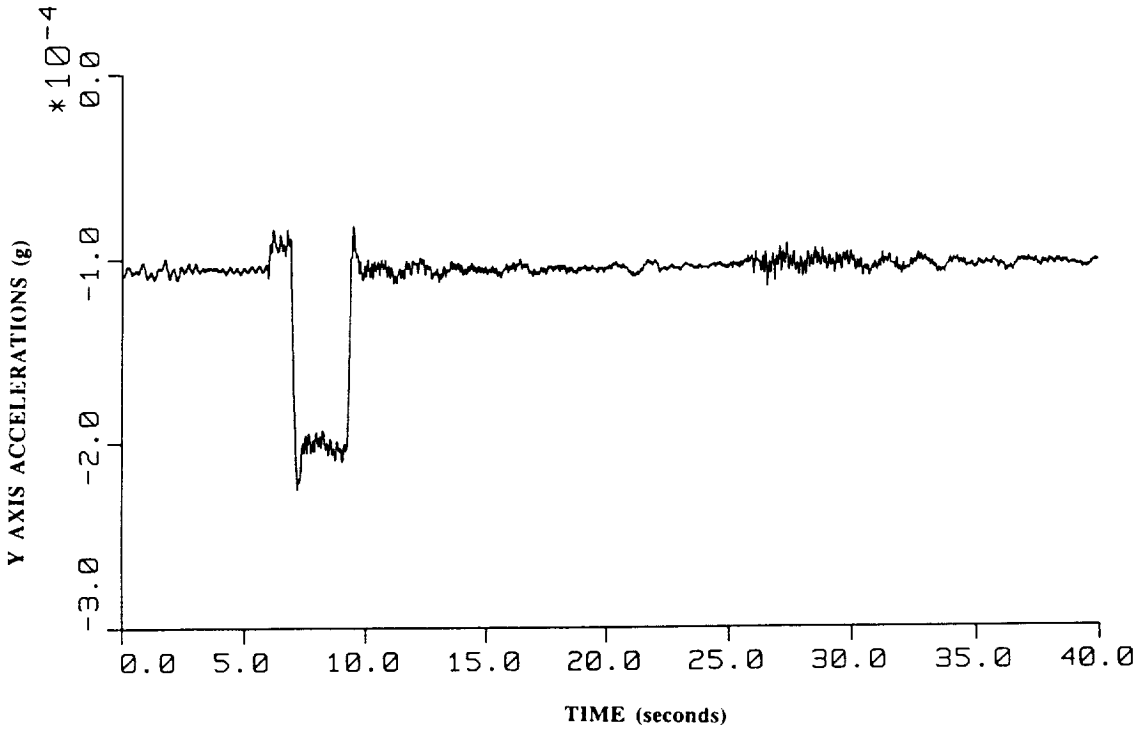

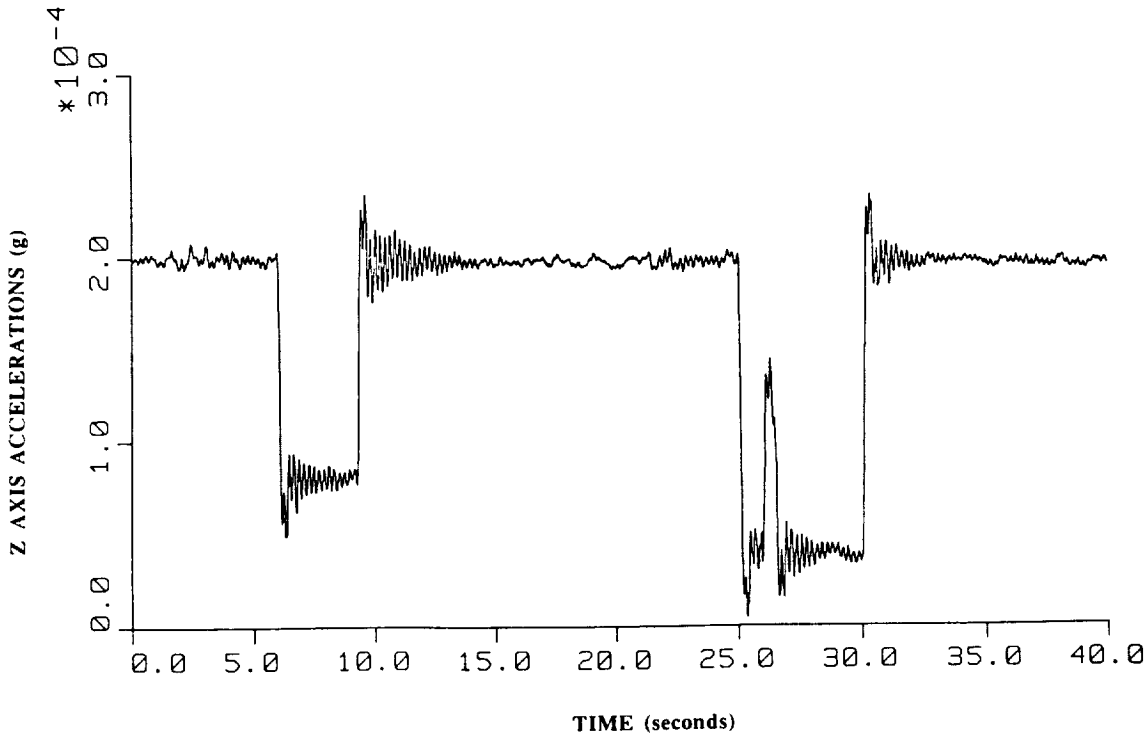

Vernier Engine Burn - multi-axis - HIRAP

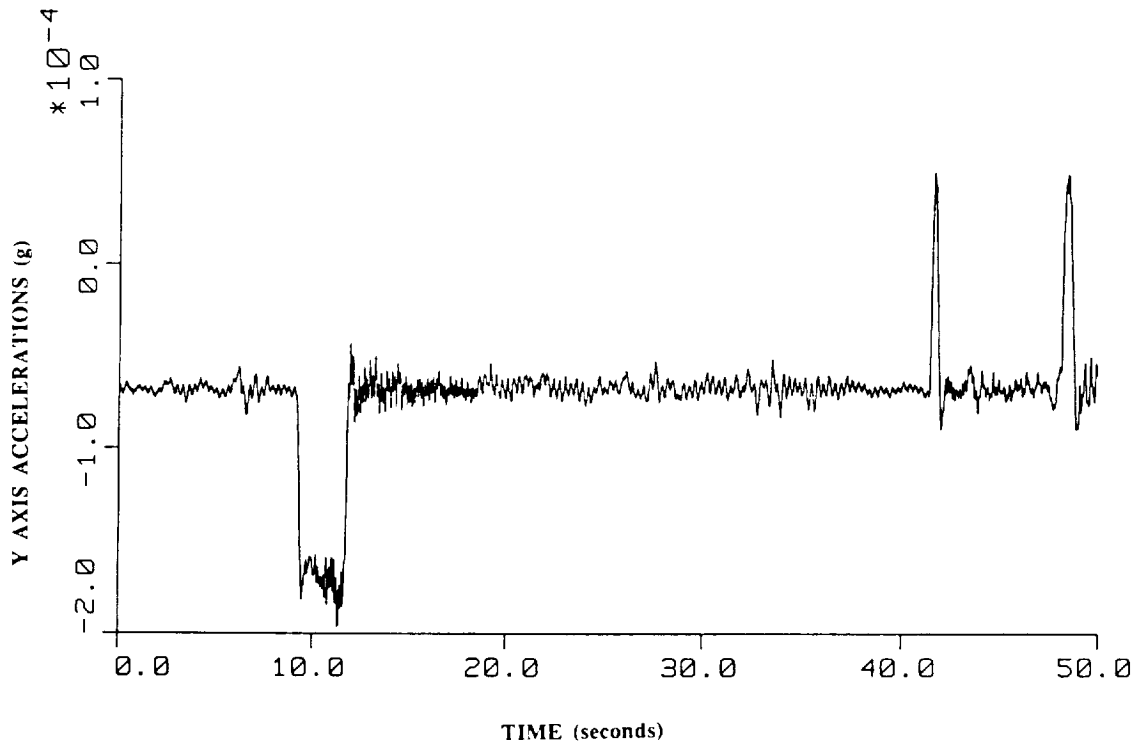

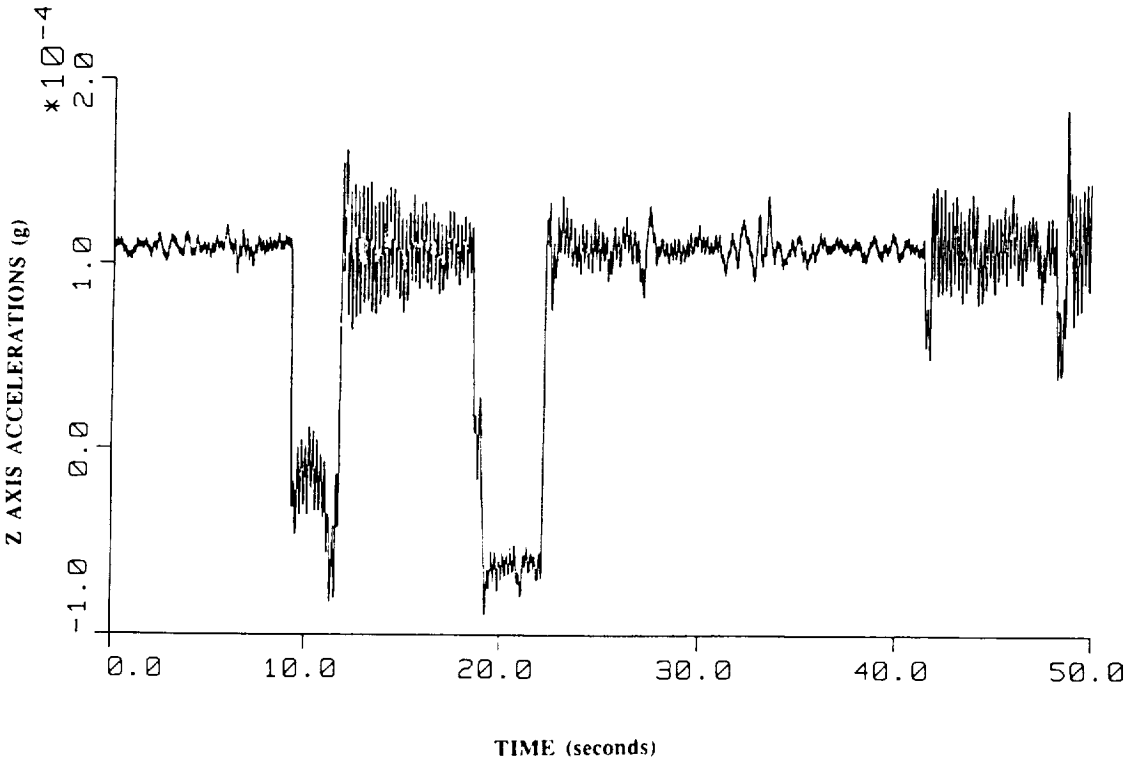

Vernier Engine Burn - multi-axis - HIRAP

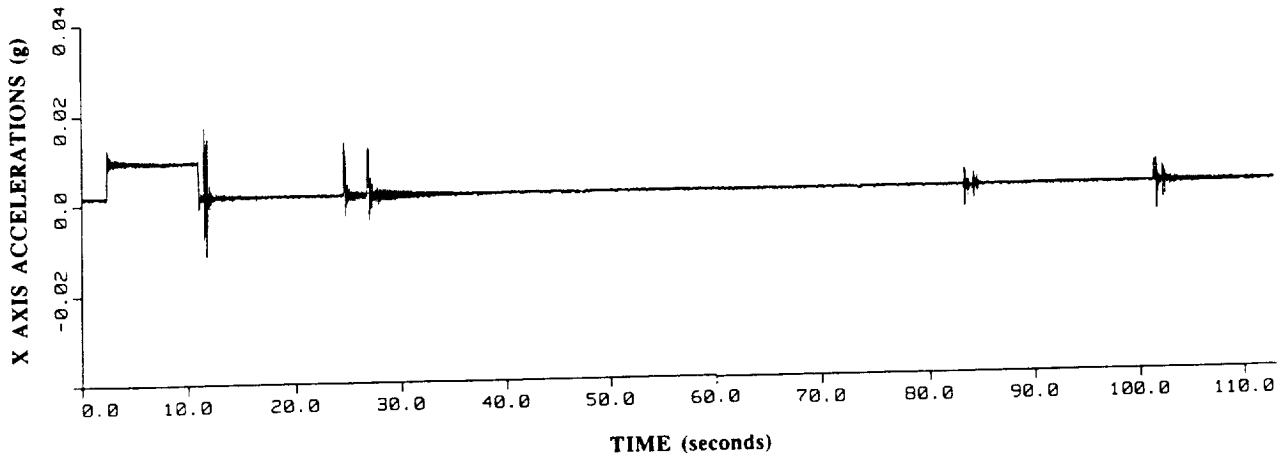

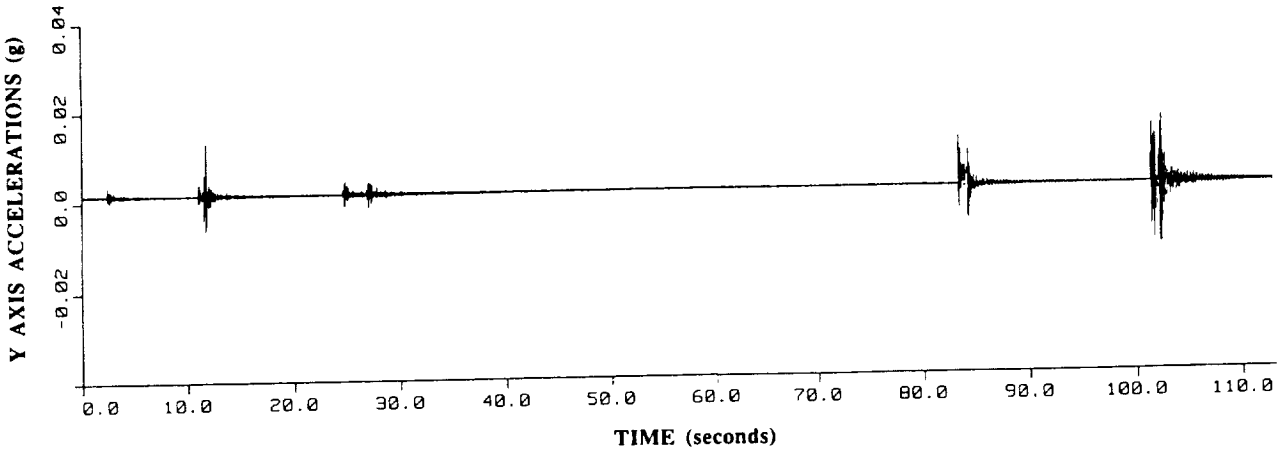

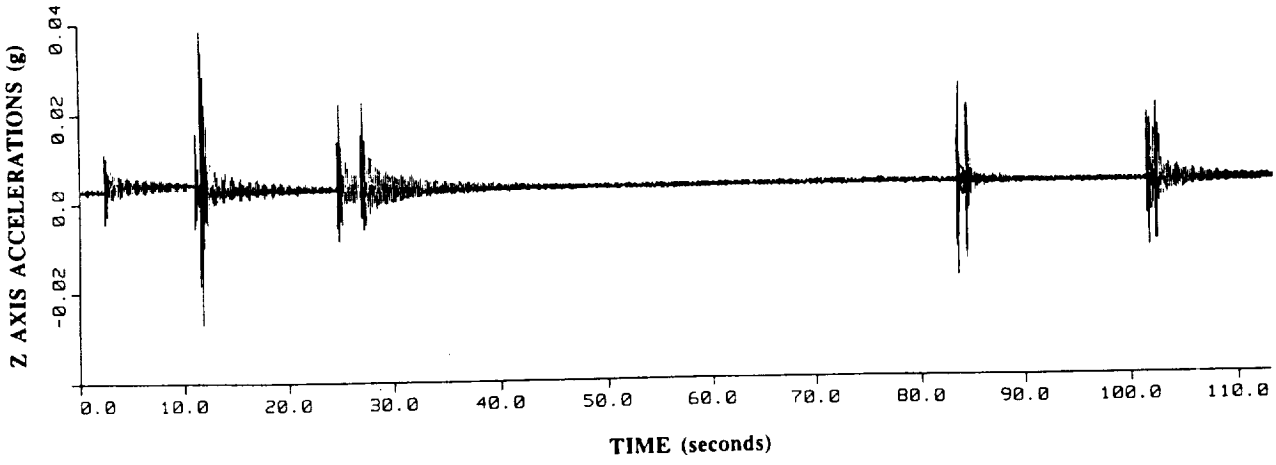

PRCS Burn - NC4 (part I) - ACIP

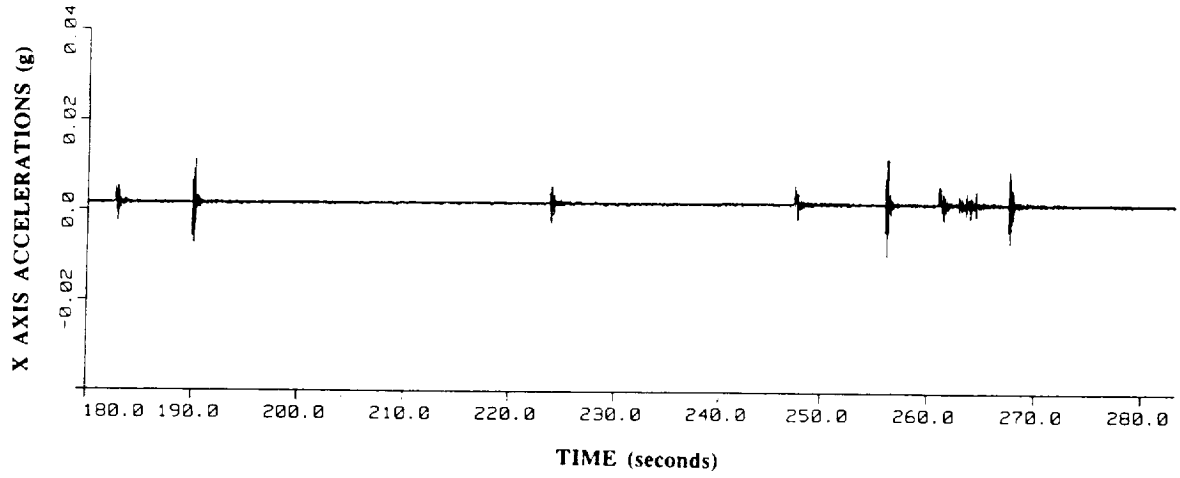

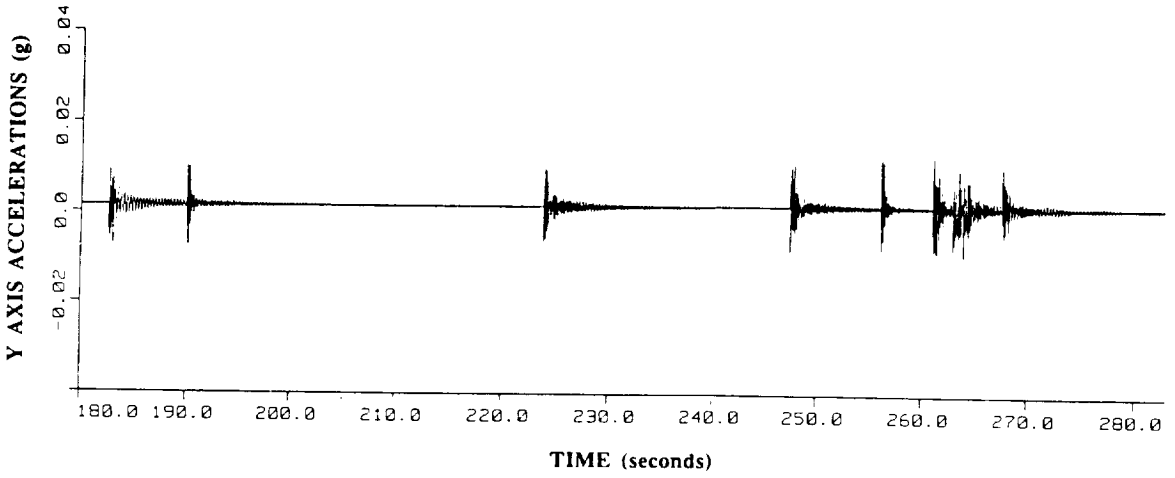

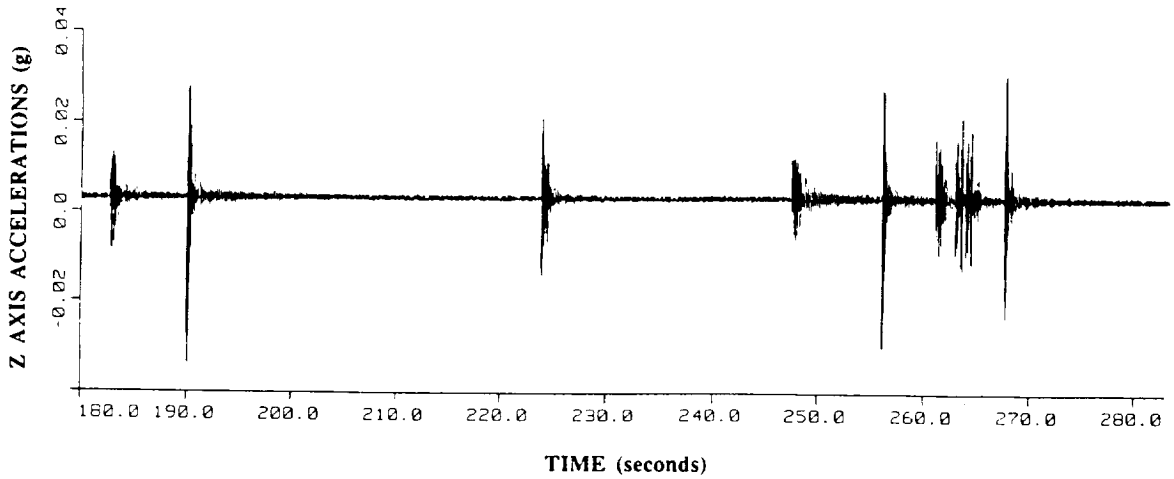

PRCS Burn - NC4 (part II) - ACIP

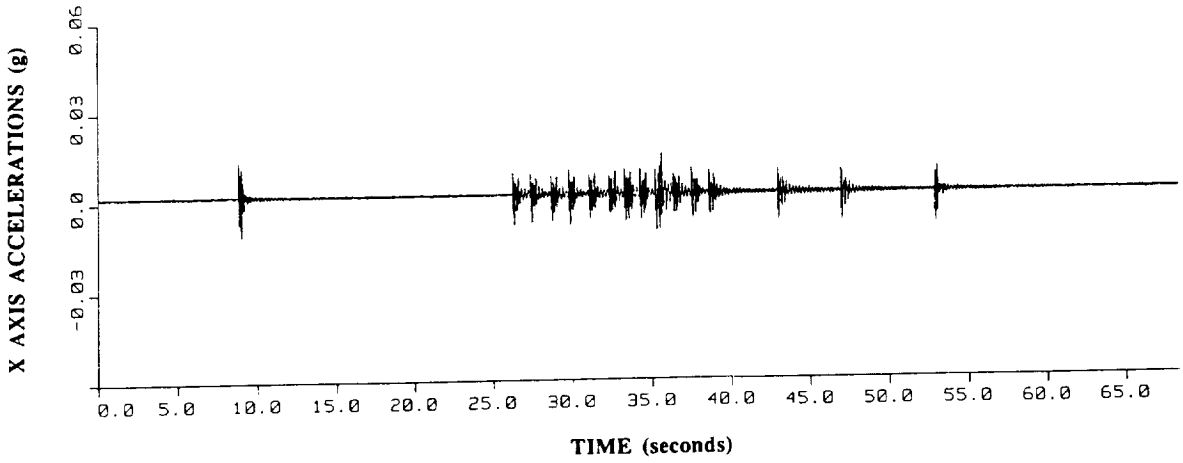

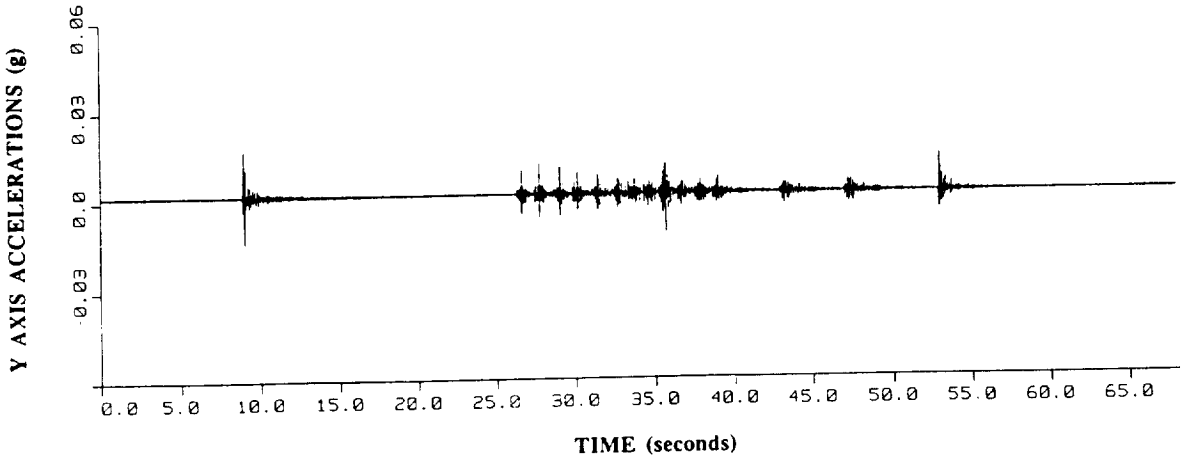

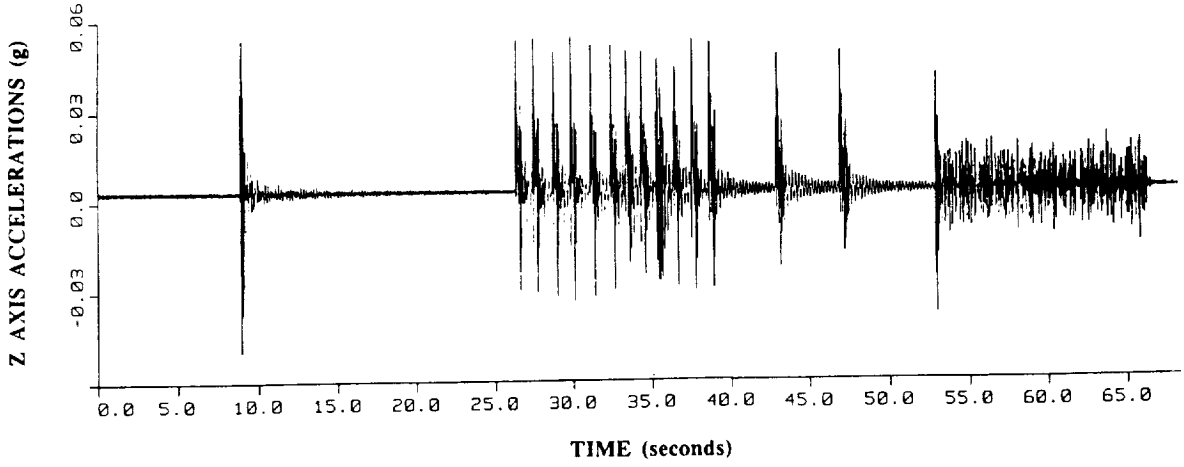

PRCS Burn - NC5 - ACIP

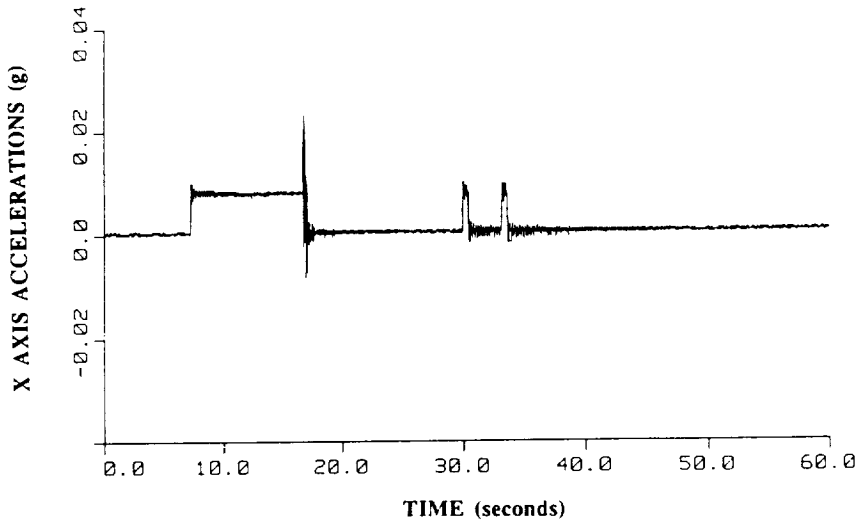

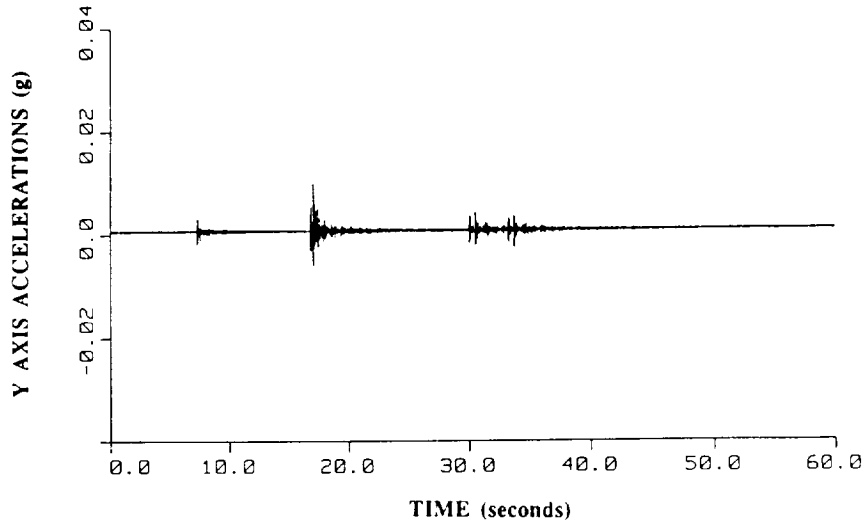

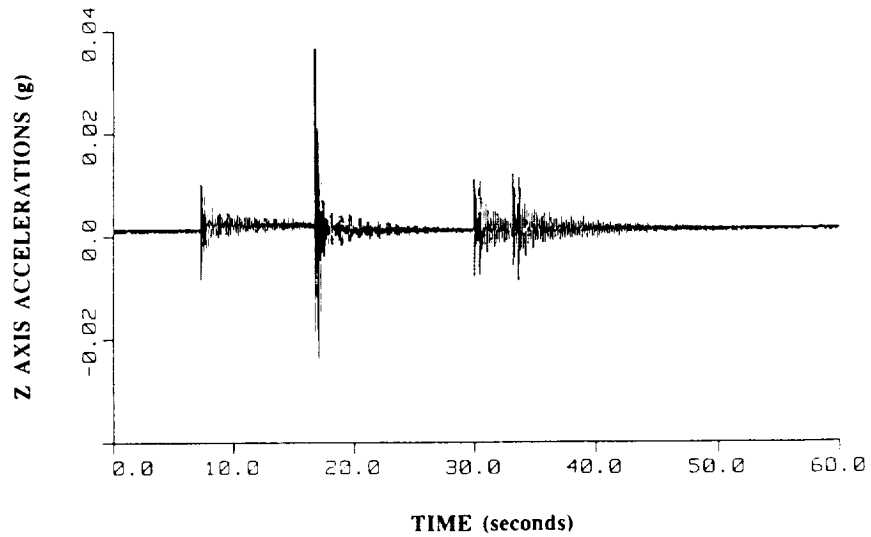

PRCS Burn - NH2 - ACIP

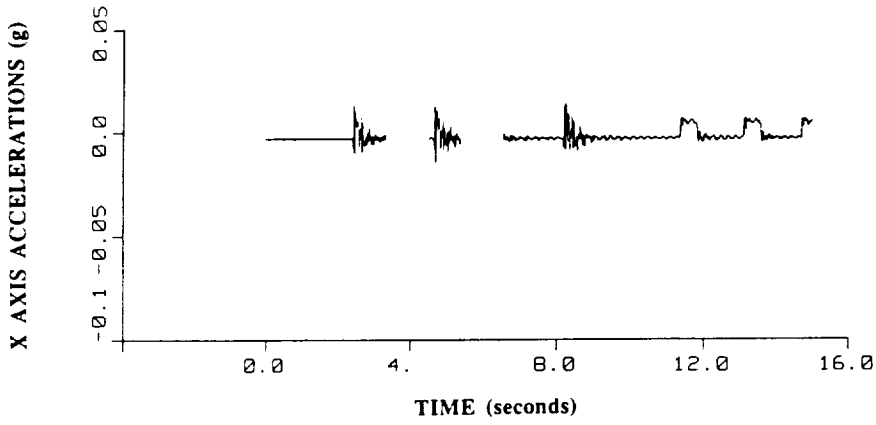

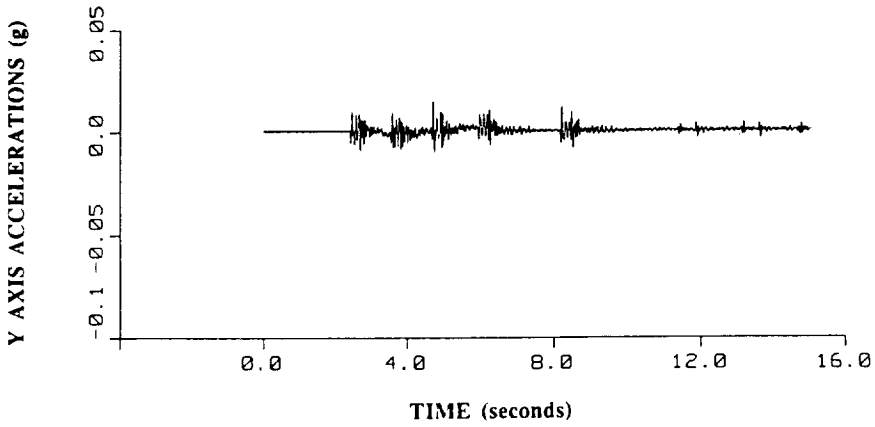

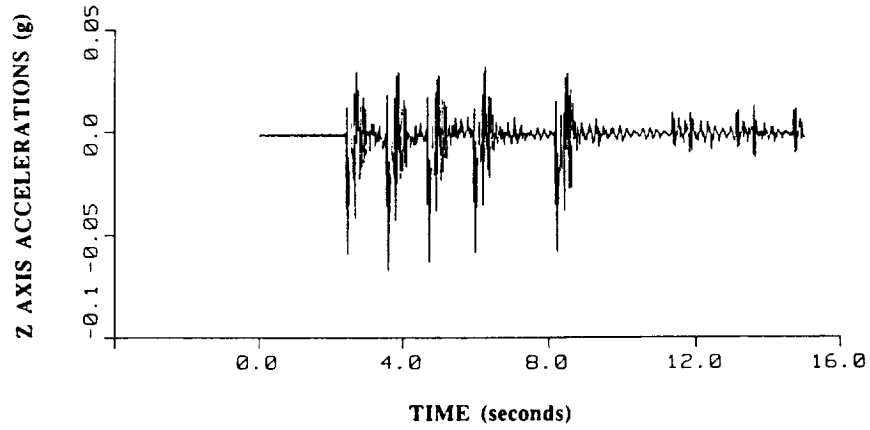

PRCS Burn - NCC - ACIP

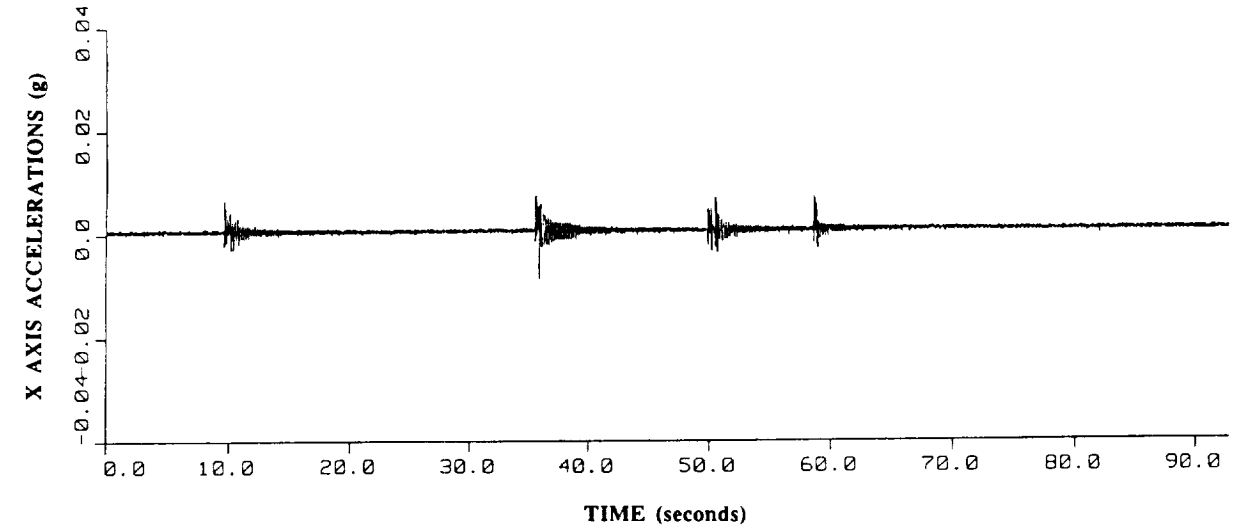

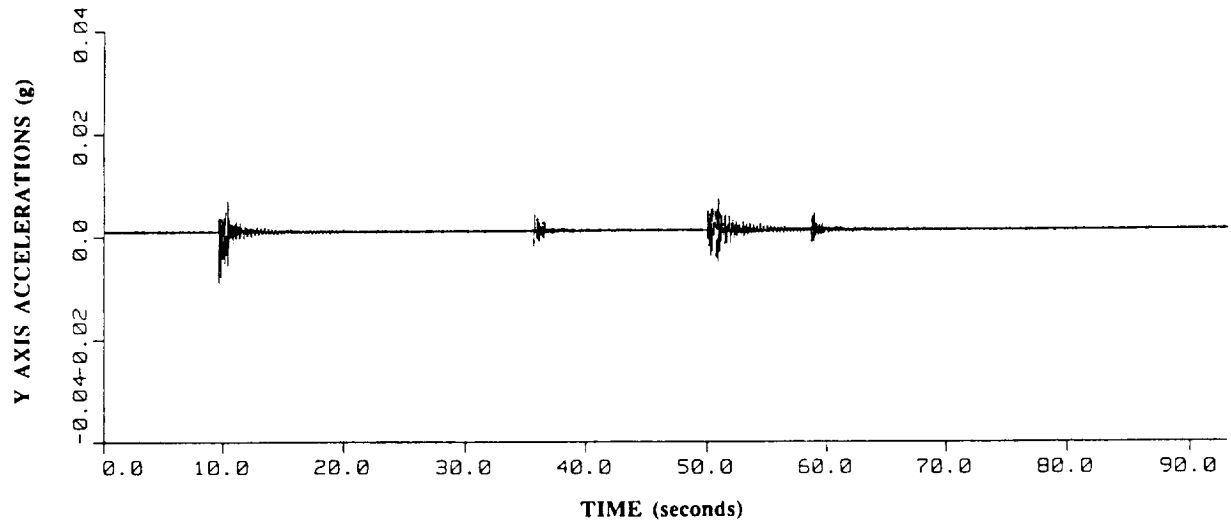

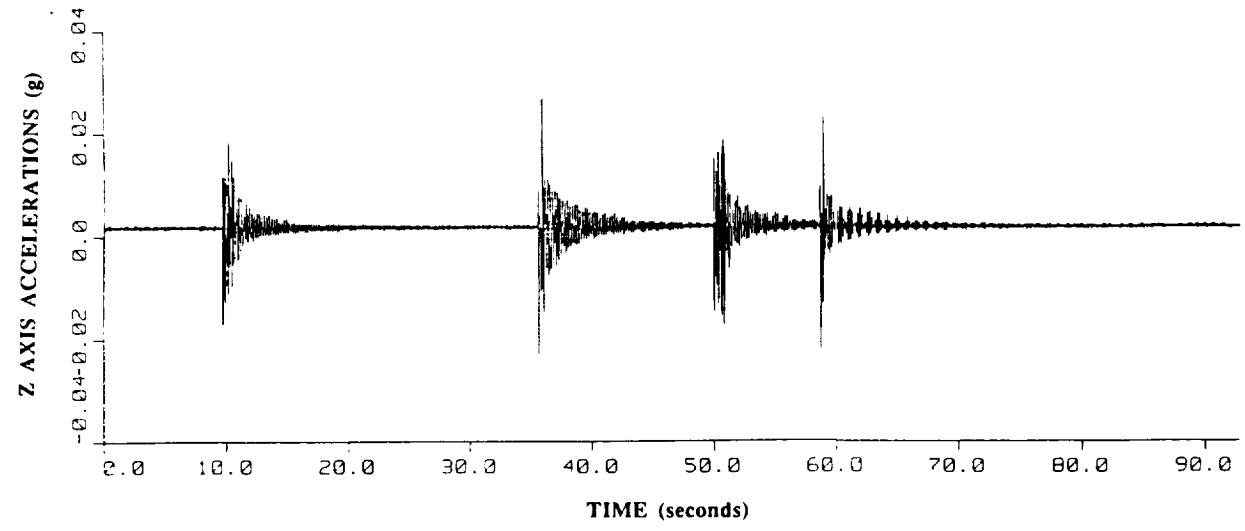

PRCS Burn - MNVR TO SEP (part I) - ACIP

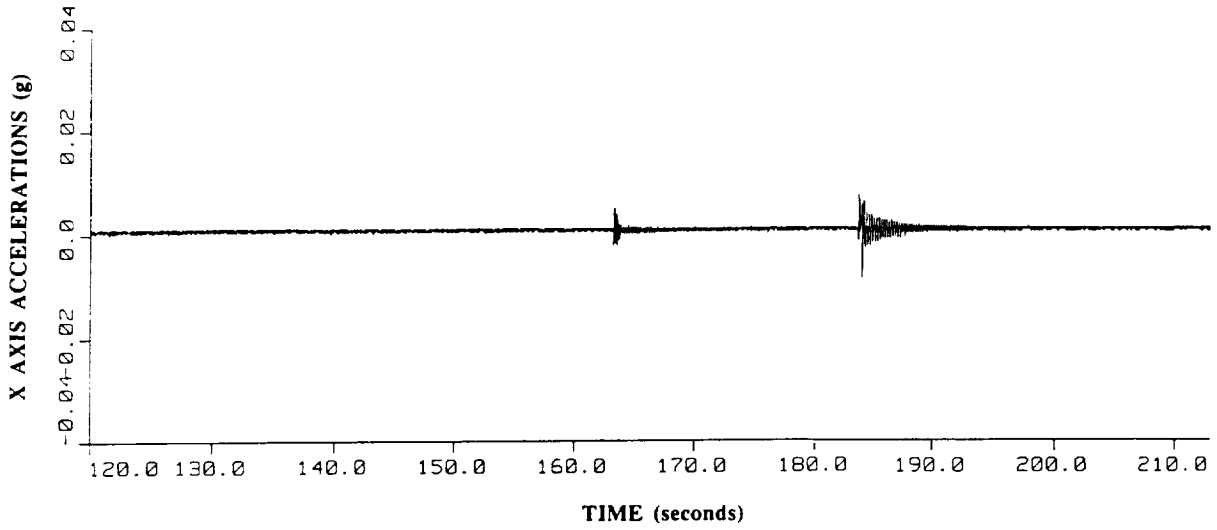

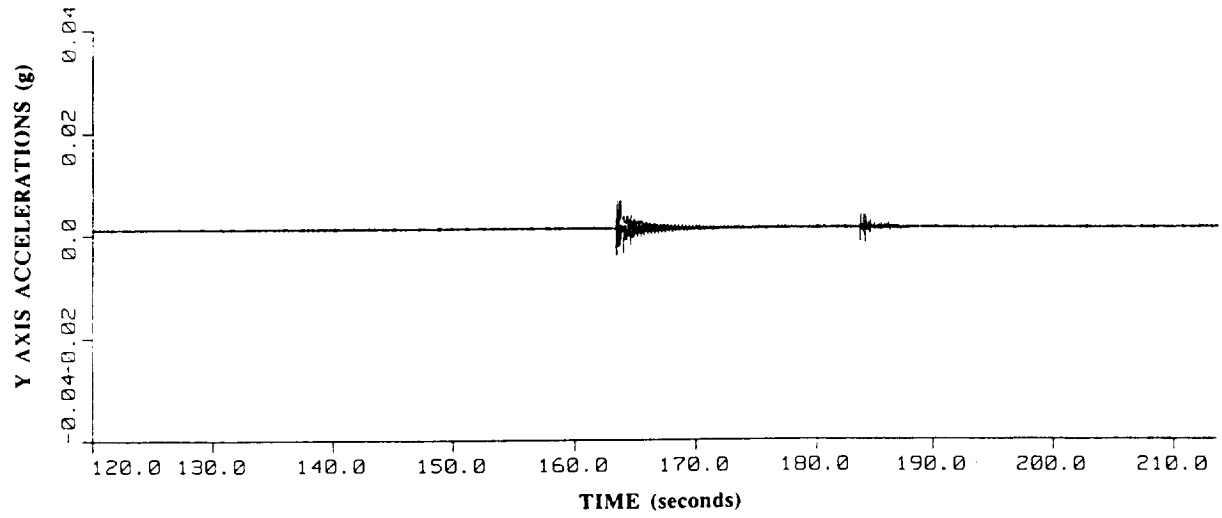

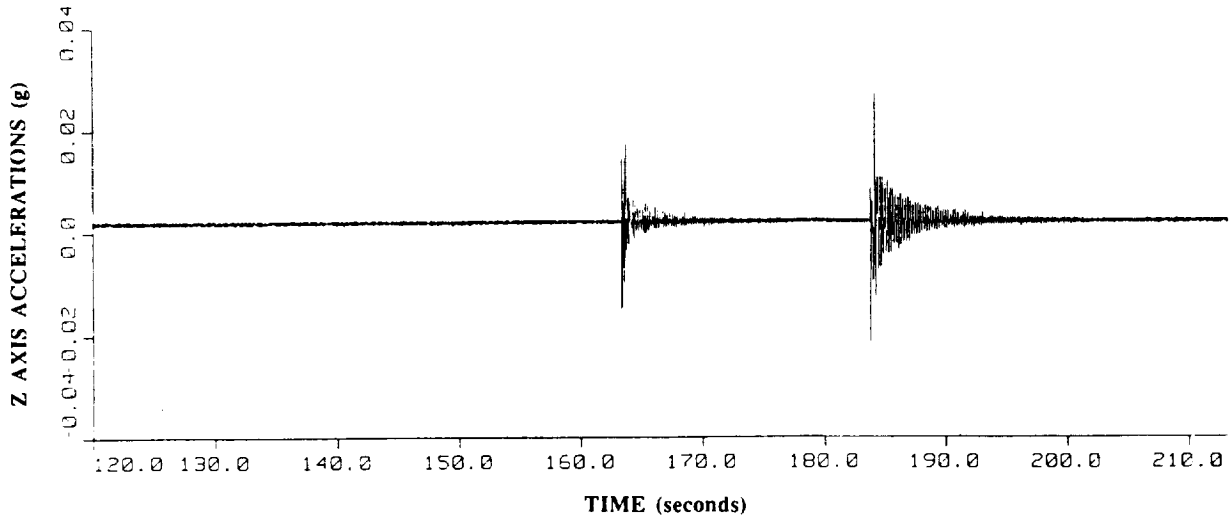

PRCS Burn - MNVR TO SEP (part II) - ACIP

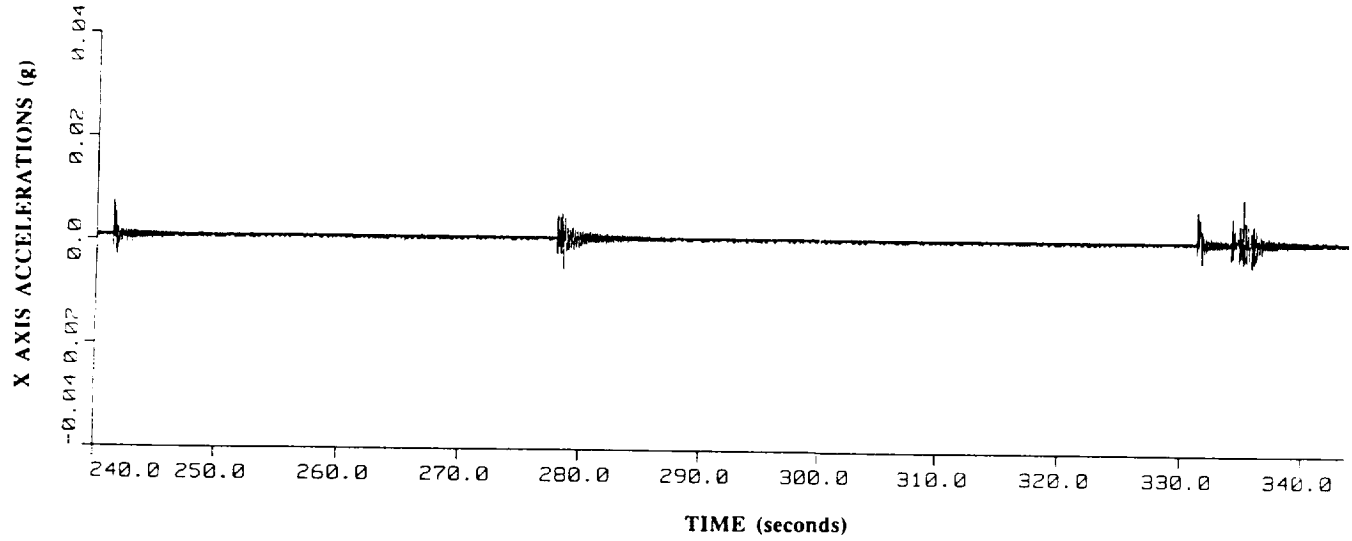

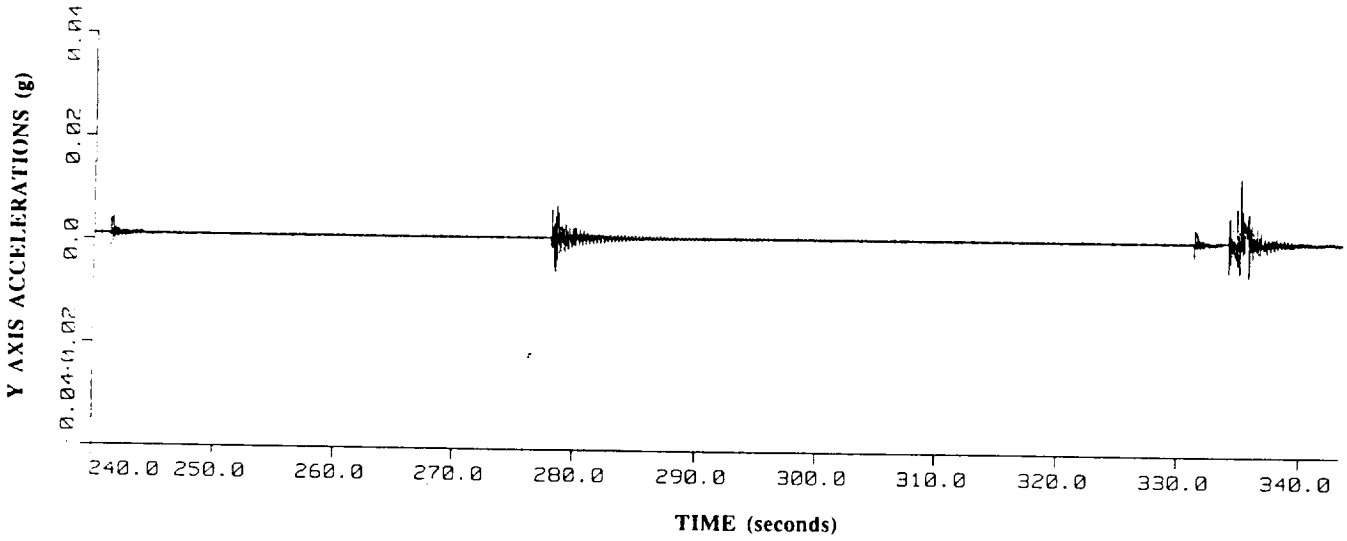

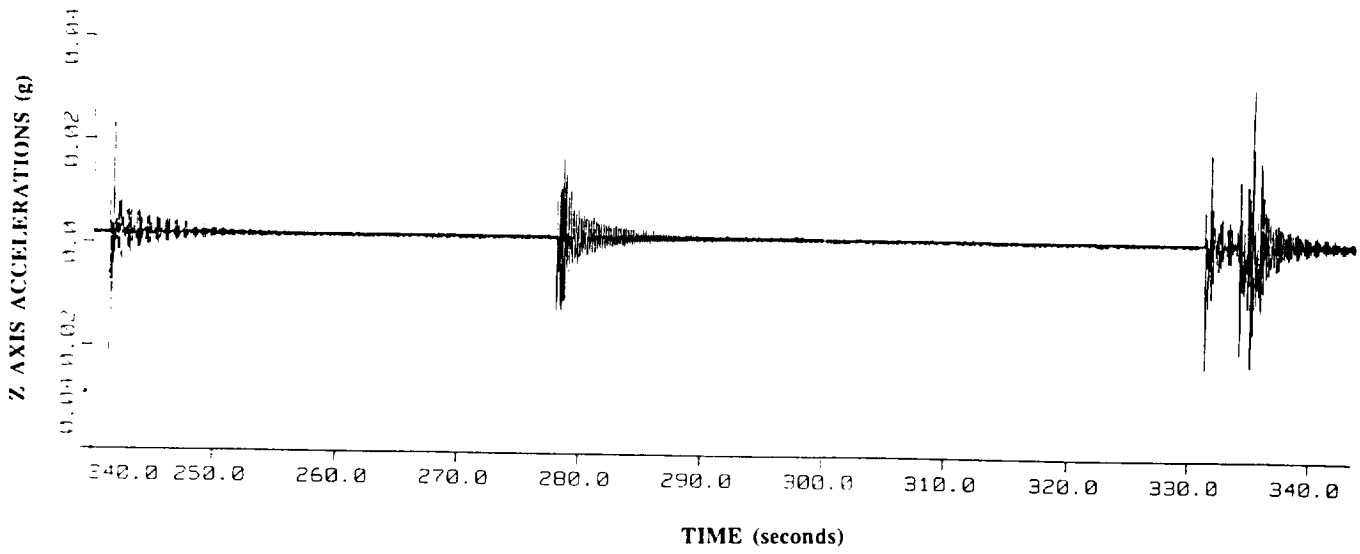

PRCS Burn - MNVR TO SEP (part III) - ACIP

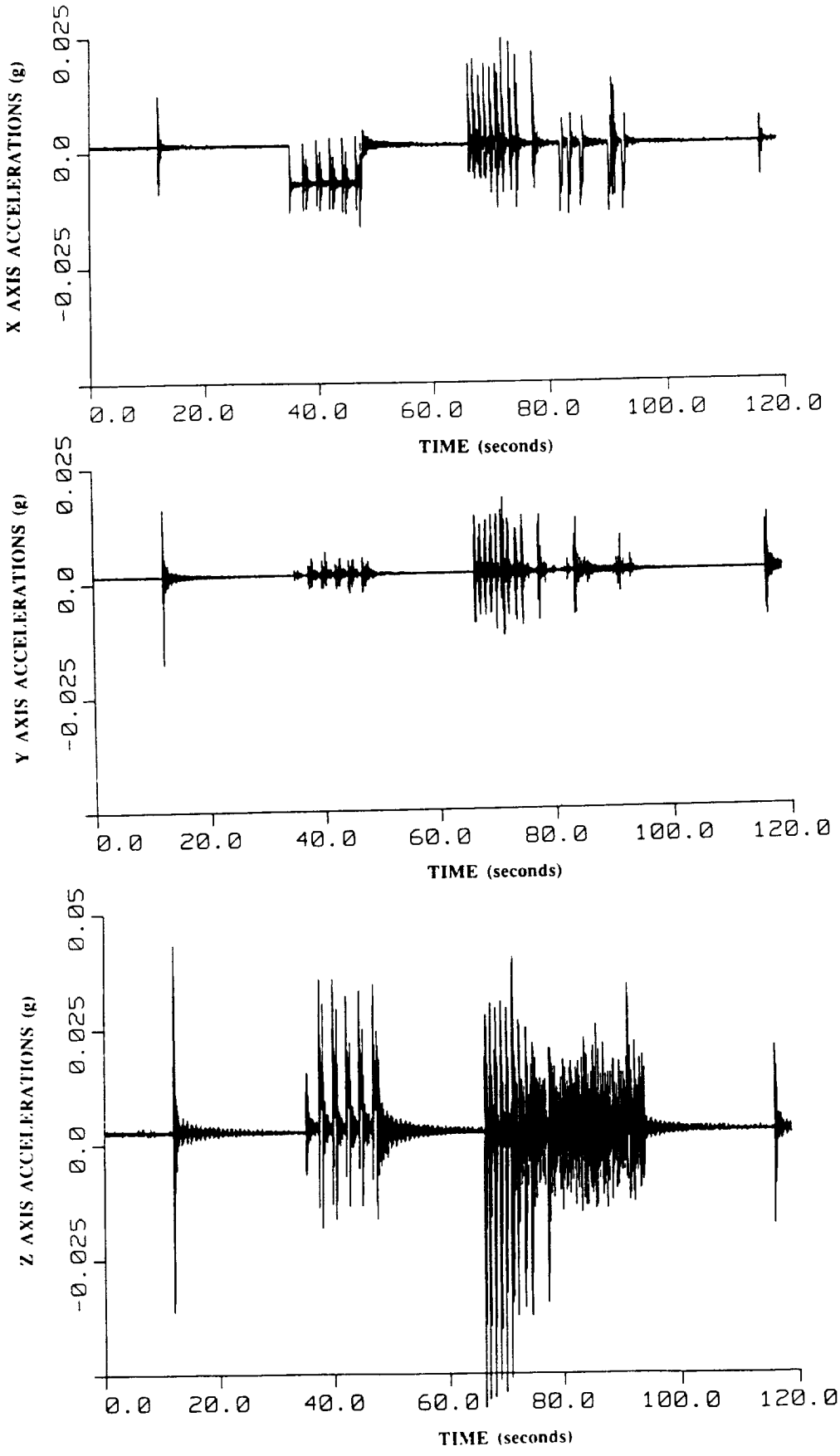

PRCS Burn - TI - ACIP

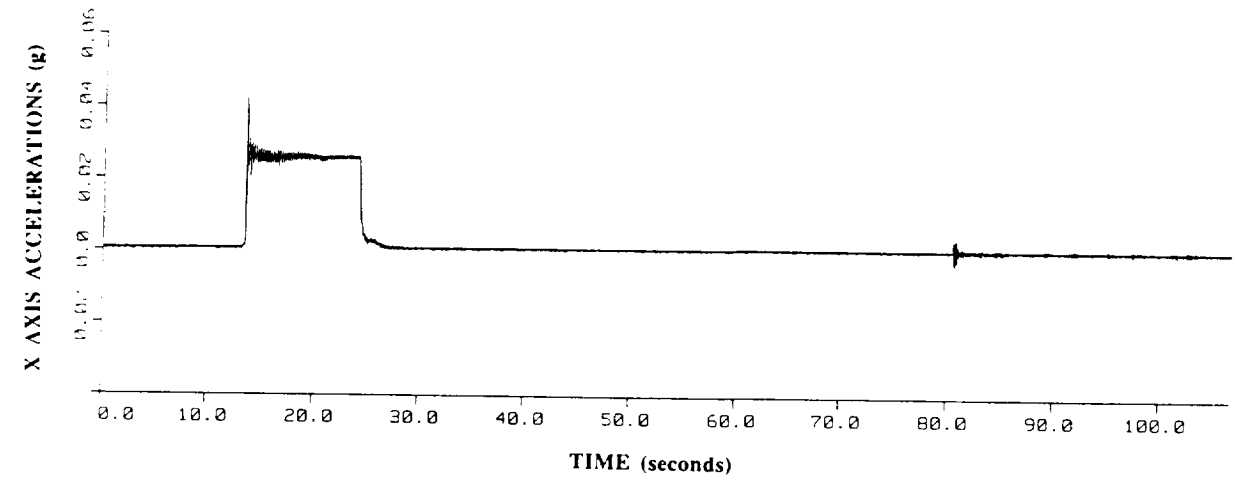

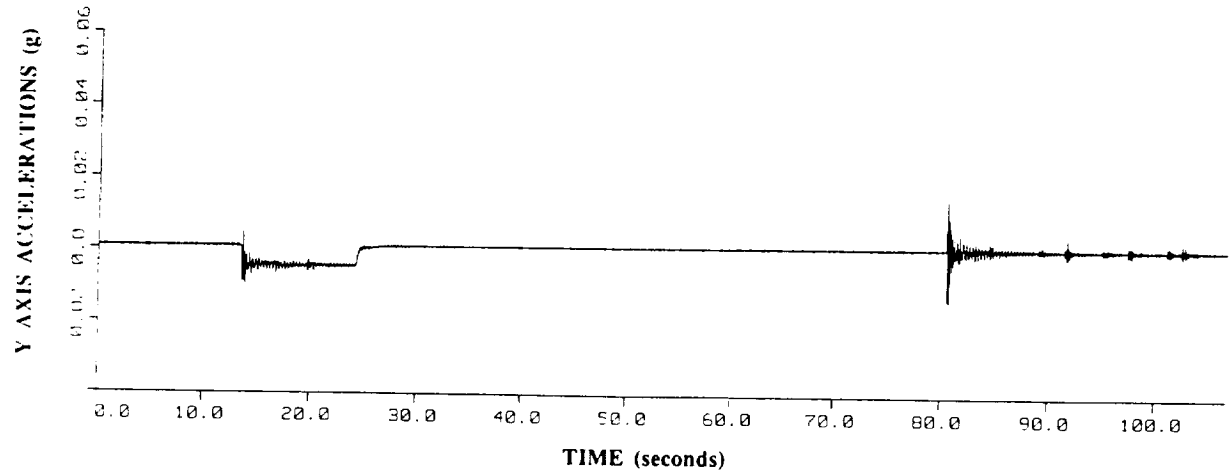

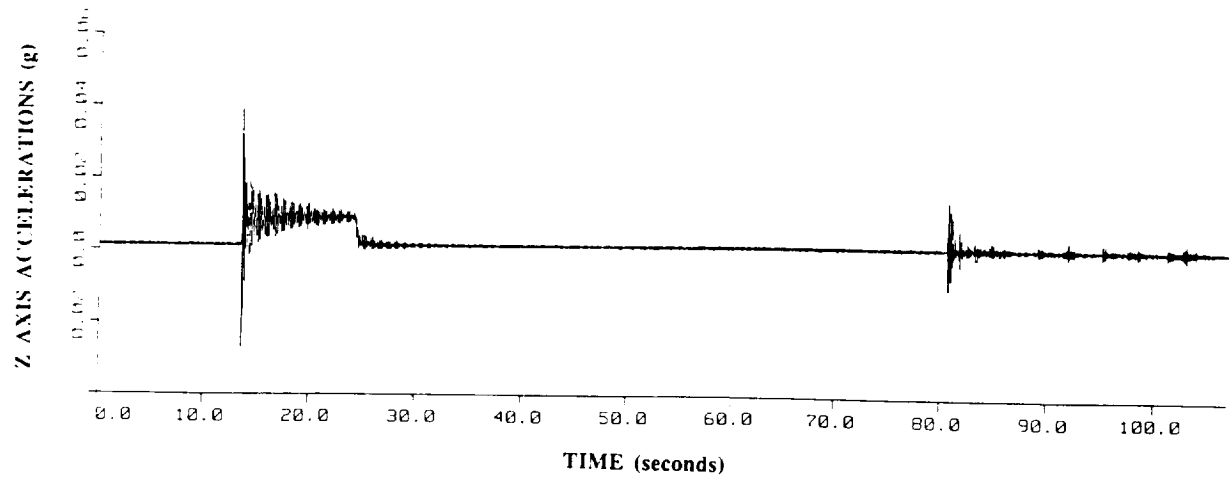

OMS Burn - NSR - ACIP

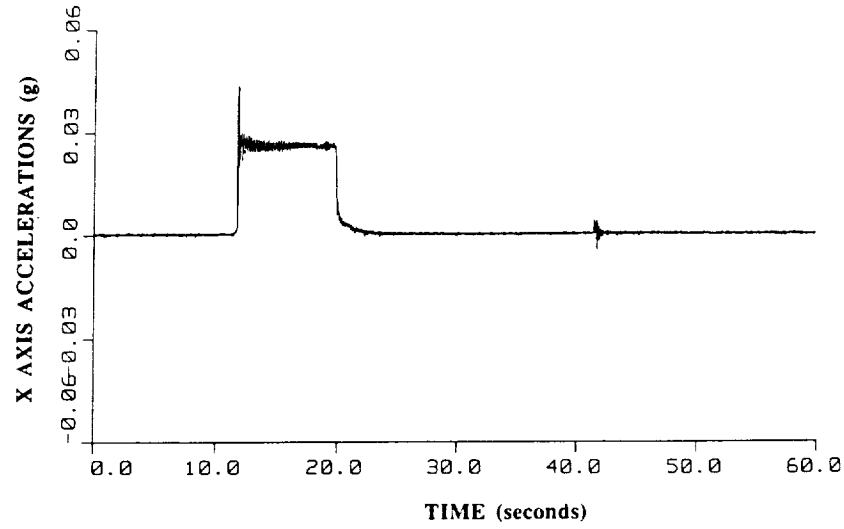

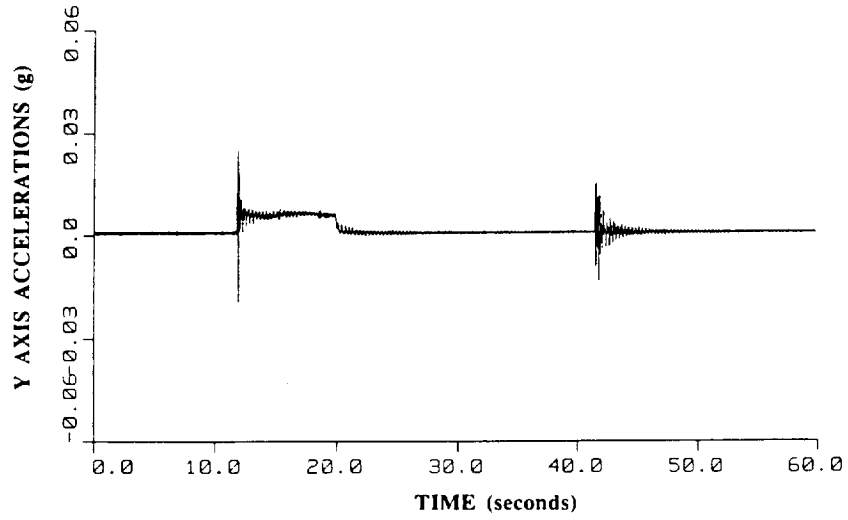

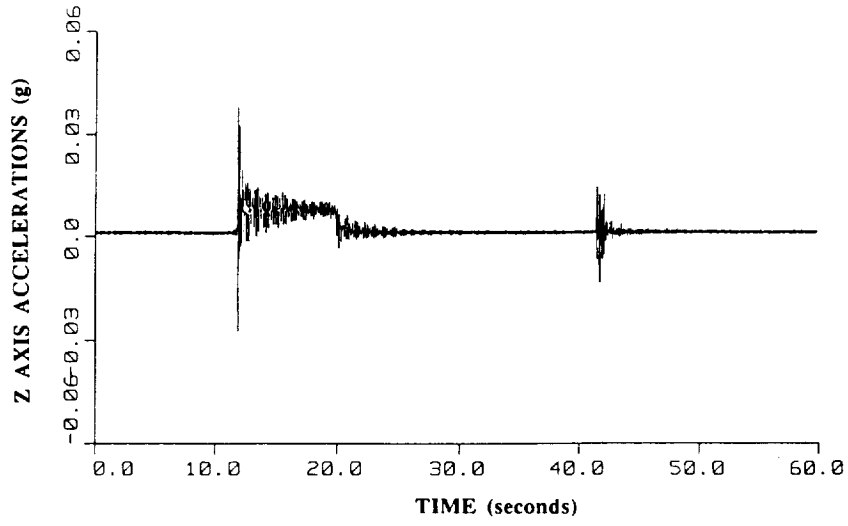

OMS Burn - NH1 - ACIP

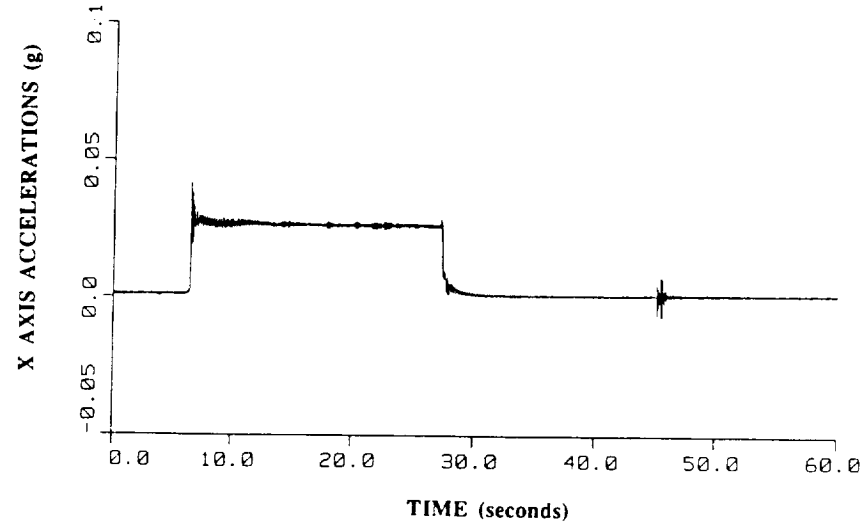

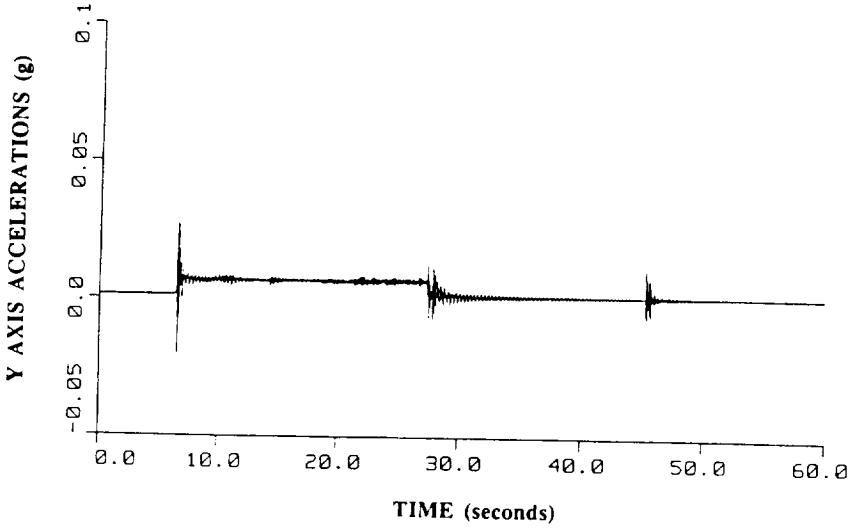

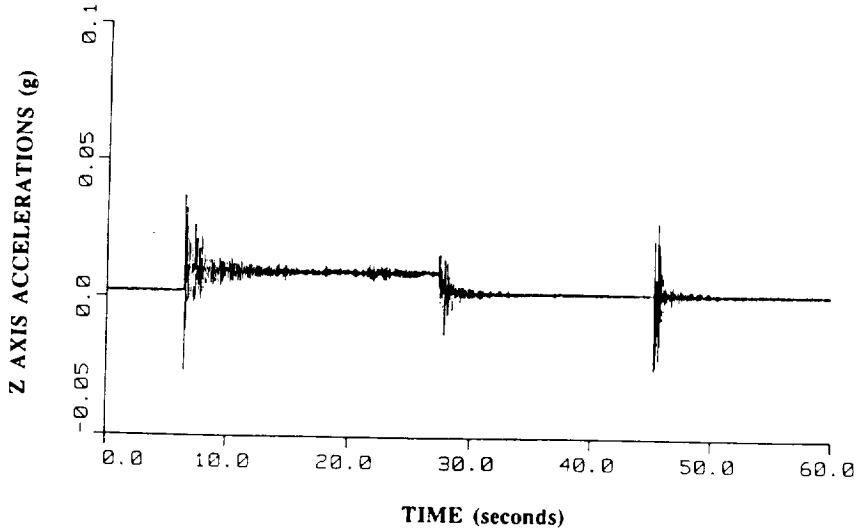

OMS Burn - SYNCOM SEP - ACIP

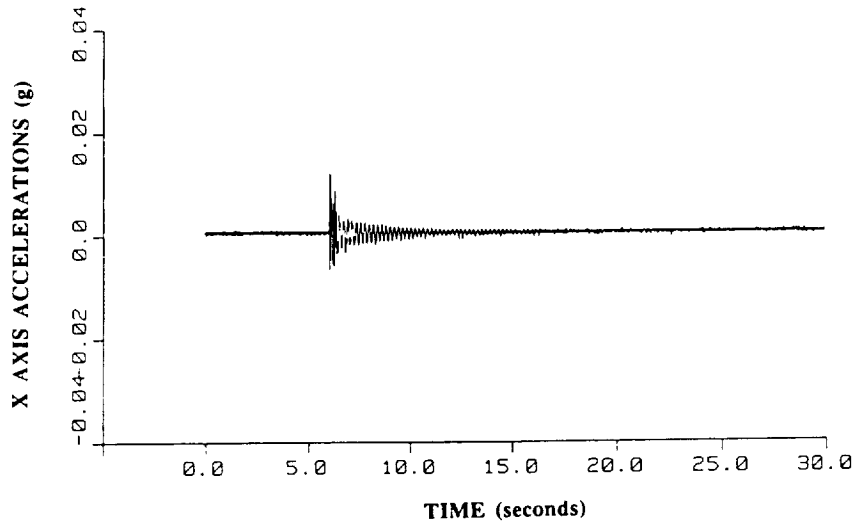

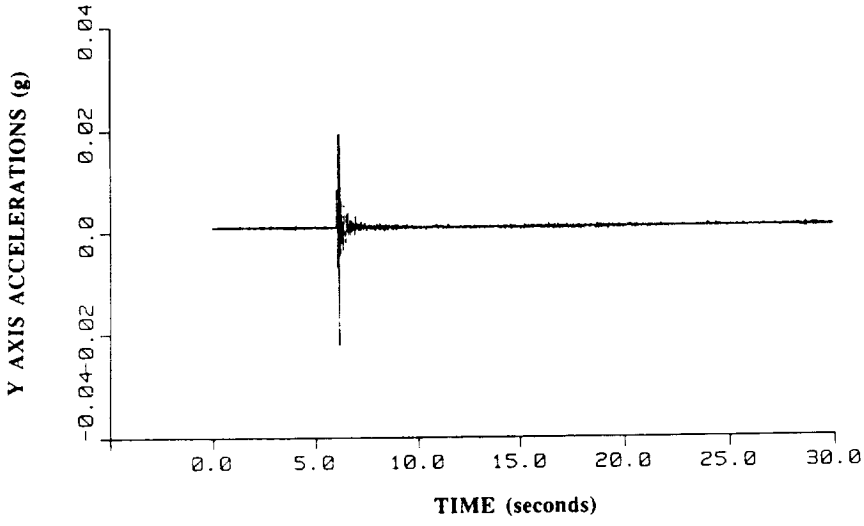

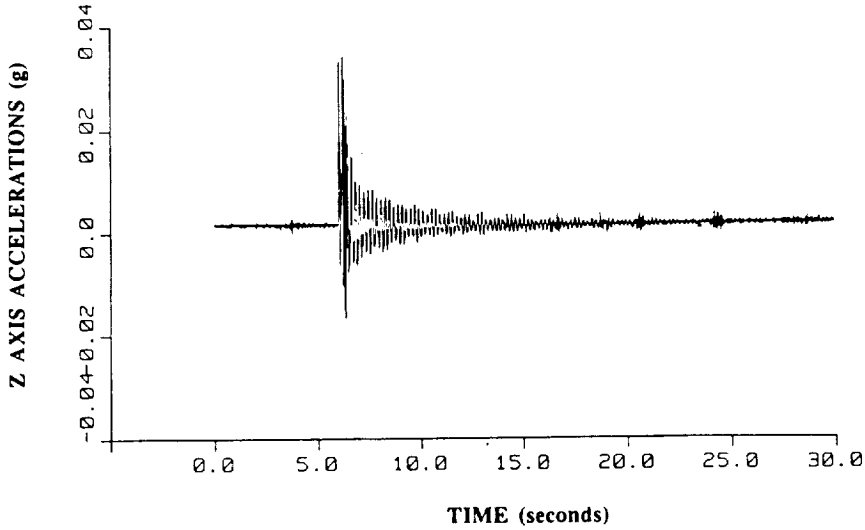

SYNCOM Deploy - ACIP

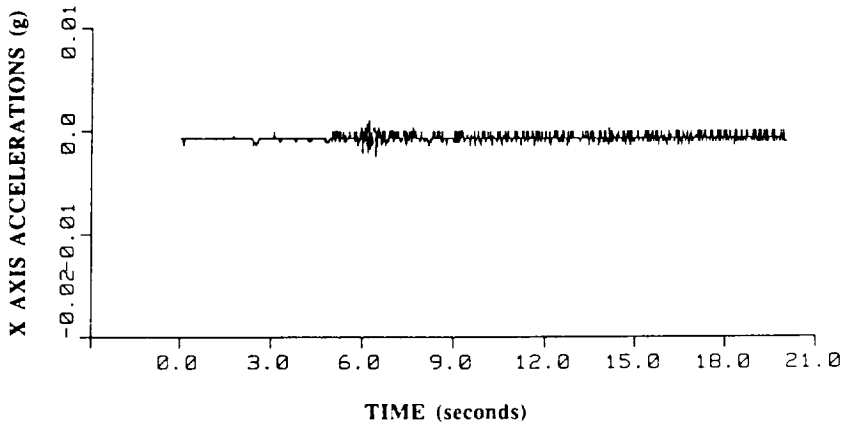

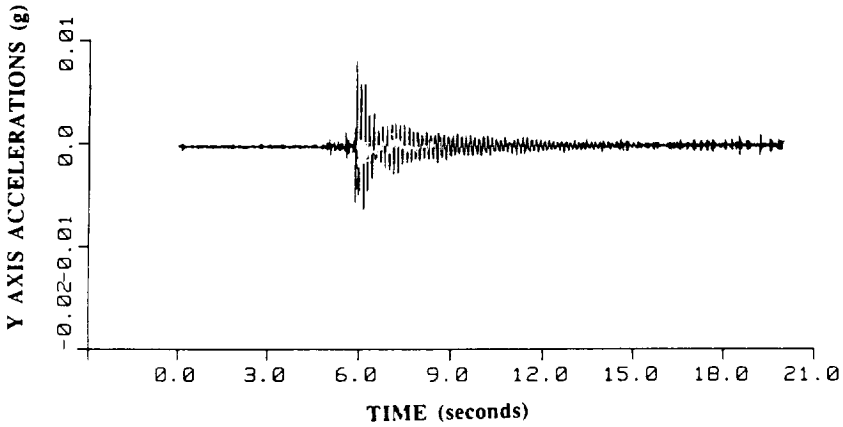

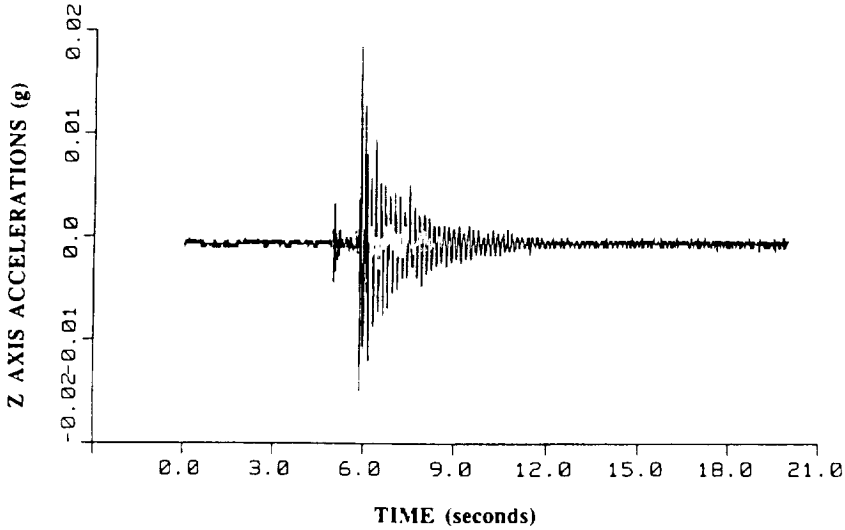

APU Startup - ACIP

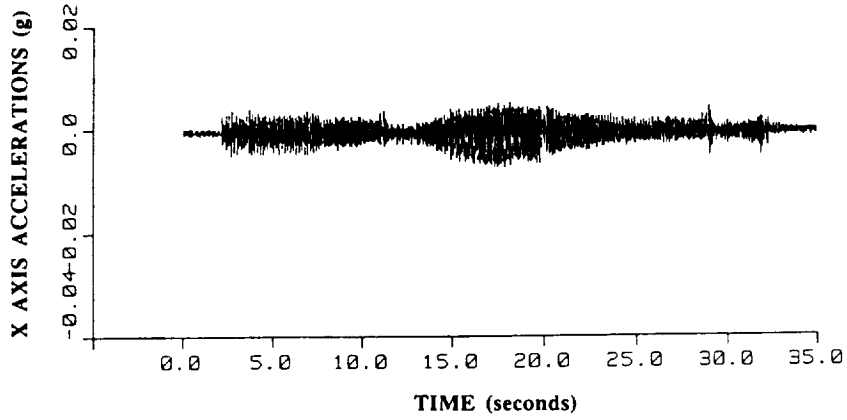

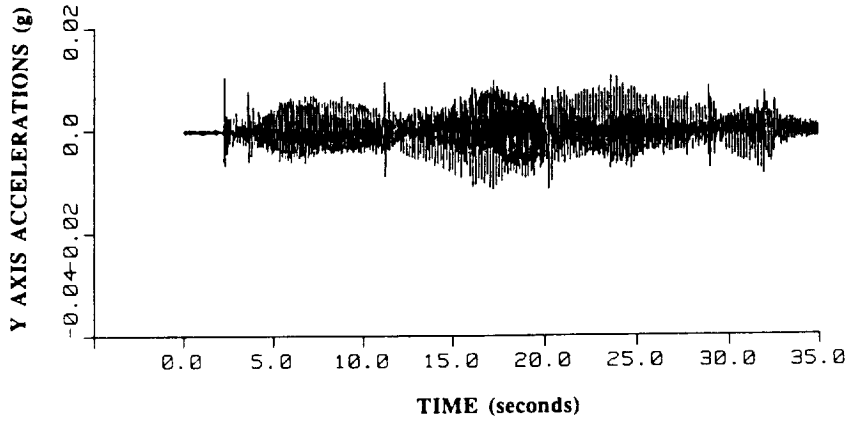

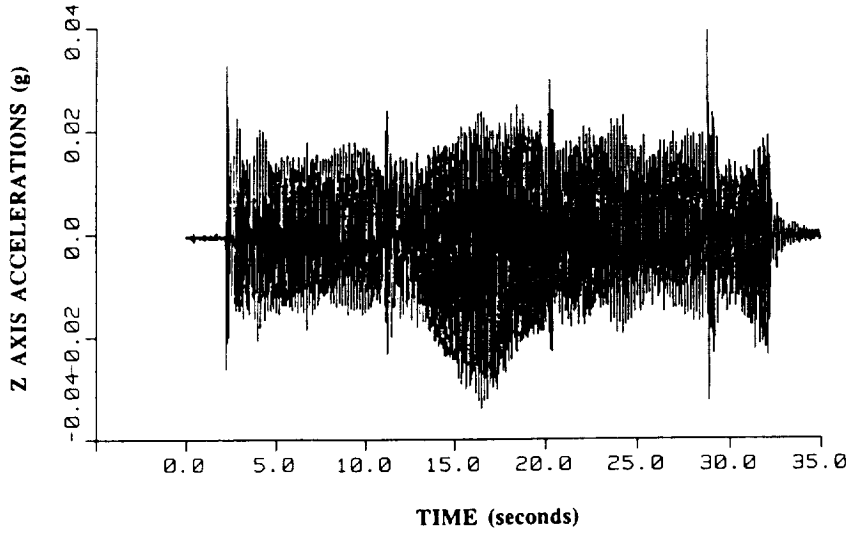

Elevon Checkout - ACIP

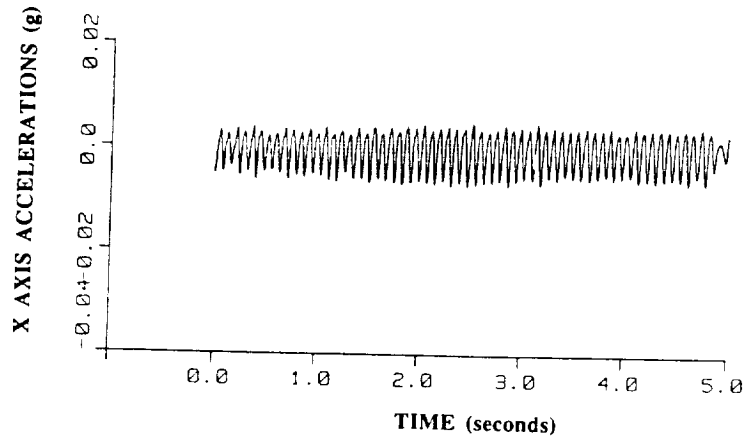

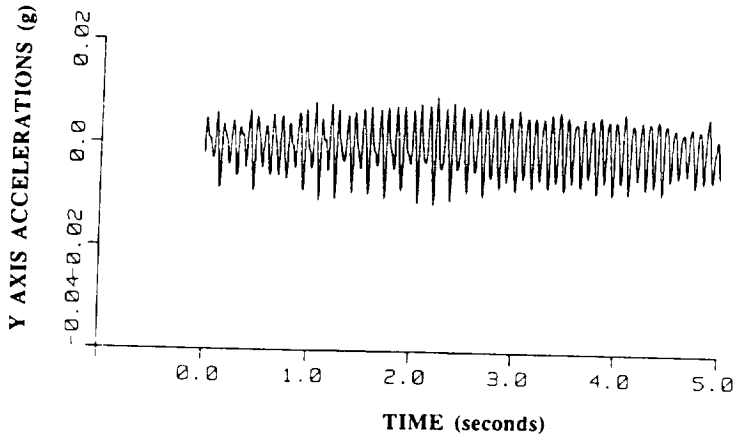

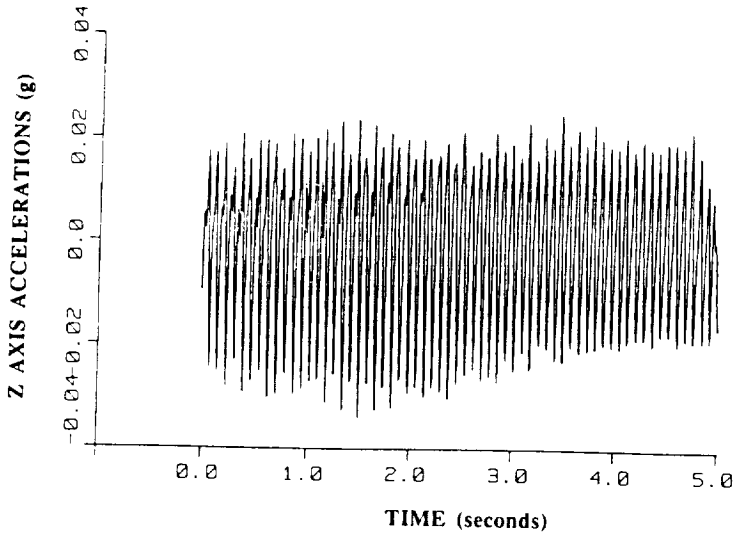

Elevon Checkout - expanded detail - ACIP

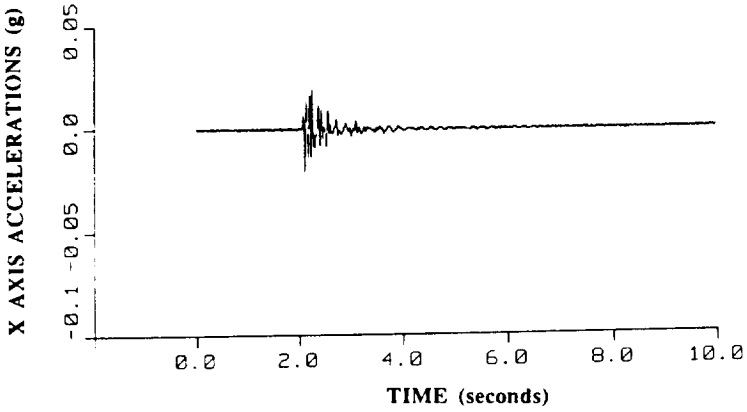

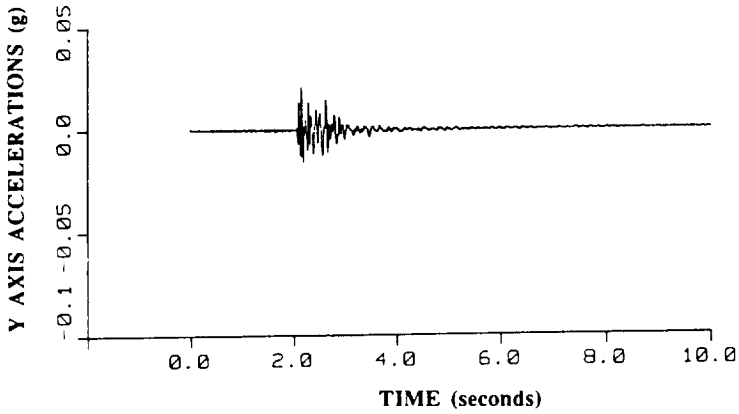

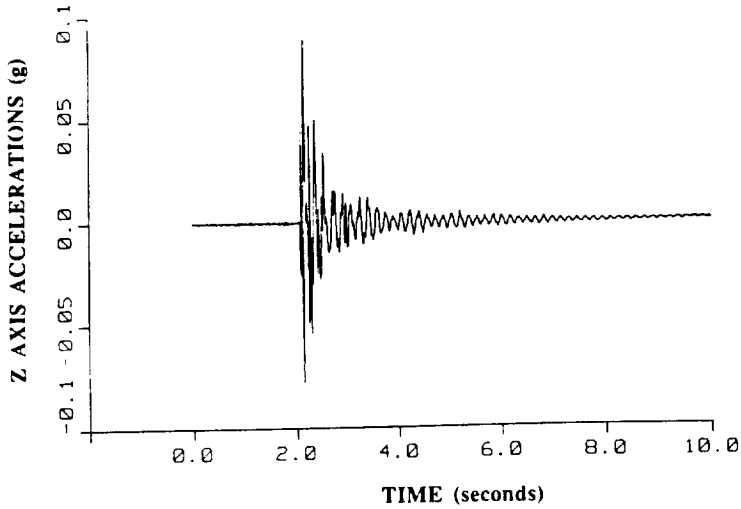

Actuator Checkout - ACIP

APPENDIX B

OMS and RCS Engines Description

Reaction Control System (RCS)

The reaction control system (RCS) consists of 44 individual thrusters located in 3 separate modules in the Orbiter (forward, aft-left, aft-right). There are 38 primary jets and 6 vernier jets. Each primary jet is rated at 870 lb. of thrust, and each vernier jet is rated at 24 lb. of thrust. The primary jets are used to control the motion of the Space Shuttle vehicle through a combination of translation and/or rotational movement. The vernier jets are only used on orbit for fine attitude control. The location of the RCS thrusters in relationship to the Orbiter is shown in figure B-1, and details of the jet locations and plume directions are shown in figure B-2. While most thrusters are aligned with the Orbiter body axes, it should be noted that many of the thrusters in the forward module are off-axis. This is further illustrated in figure B-3. The six vernier thrusters are shown on figure B-2 as F5R, F5L, L5L, L5D, R5R, and R5D.

Orbital Maneuvering System (OMS)

The OMS engines provide propulsion for the Space Shuttle vehicle during the orbit phase of flight. They are used for orbital insertion maneuvers after the main propulsion system has shut down. They are also the primary propulsion system for orbital transfer maneuvers and the deorbit maneuver.

There are two OMS engines per Orbiter. Each OMS engine produces 6000 lb. of thrust. The location of the OMS engines in relationship to the Orbiter is shown in figure B-1. As shown in figure B-4, the OMS engines are canted 15.8° upward and 6.5° outboard with respect to the Orbiter body axes. The OMS engines can be pivoted up and down ($\pm 6°$) and from side to side ($\pm 7°$) from their null position.

Orbiter Engine Burn Designations

The four PRCS burn designations (NCC, TI, MC3, and MC4) and two OMS burn designations (NH1 and NSR) listed in table 3 are specific types of engine burns performed during nominal Orbiter rendezvous operations and were executed on STS-32 during the LDEF rendezvous sequence. A brief description of each is provided.

NCC - The NCC burn is used to correct the Orbiter trajectory to achieve a desired offset position from the target. It is usually a combination of three maneuvers and is the first onboard targeted burn using sensor data.

TI - The TI burn is one of the final burns in the rendezvous sequence and is also known as the target intercept burn.

MC - The MC burns (MC1, MC2, MC3, MC4) are a series of burns used as mid-course corrections to intercept the final target. These burns would generally follow the TI burn.

NH - The NH burn is a height adjustment burn and is generally a posigrade or retrograde burn.

NSR - The NSR burn is used to enter a co-eliptical orbit with the target. There is generally one NSR burn per rendezvous.

NC - The NC burn is a "catch-up" or phasing burn used to close in on the target. There are generally several of these per rendezvous (NC1, NC2, NC3, etc.)

Figure B-1. Reaction Control Subsystems